

---

Masters Theses

Student Theses and Dissertations

---

Fall 1997

## Stemming technique for loading angled holes charged with ANFO

Michael David Wilkins

Follow this and additional works at: [https://scholarsmine.mst.edu/masters\\_theses](https://scholarsmine.mst.edu/masters_theses)



Part of the [Explosives Engineering Commons](#)

Department:

---

### Recommended Citation

Wilkins, Michael David, "Stemming technique for loading angled holes charged with ANFO" (1997).  
*Masters Theses*. 1678.

[https://scholarsmine.mst.edu/masters\\_theses/1678](https://scholarsmine.mst.edu/masters_theses/1678)

This thesis is brought to you by Scholars' Mine, a service of the Missouri S&T Library and Learning Resources. This work is protected by U. S. Copyright Law. Unauthorized use including reproduction for redistribution requires the permission of the copyright holder. For more information, please contact [scholarsmine@mst.edu](mailto:scholarsmine@mst.edu).

**STEMMING TECHNIQUE FOR LOADING ANGLED HOLES CHARGED  
WITH ANFO**

**BY**

**MICHAEL DAVID WILKINS, 1972-**

**A THESIS**

**Presented to the Faculty of the Graduate School of the**

**UNIVERSITY OF MISSOURI – ROLLA**

T7380  
91 pages


**in Partial Fulfillment of the Requirements for the Degree**

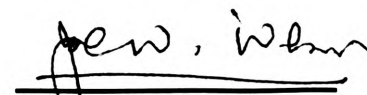
**MASTER OF SCIENCE**

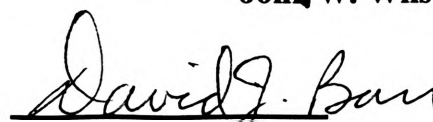
**in**

**MINING ENGINEERING**

**1997**

  
**Paul N. Worsey**

  
**John W. Wilson**

  
**David J. Barr**

## ***ABSTRACT***

Little research has been published on stemming blast holes, particularly what happens during the process. Previous work has concentrated on the performance of the inert material to find the best way to seal the hole and retain the explosive energy, at the exclusion of determining what happens during the loading and stemming process. Such studies were carried out by Konya and Worsey.

The major problem with stemming studies is that rock is an opaque material, and the actual mechanisms involved during the stemming process cannot be viewed. For this reason, tests were performed using clear tubes to simulate a blast hole with ANFO used as the explosive. The tests incorporated three or more different hole angles, three different tube sizes, three or more flow rates for both ANFO and stemming, and four types of stemming. A video camera was used to record each test. It was found that complex interfaces developed between the ANFO and stemming depending upon the hole angle and the flow rate of the stemming. Fast stemming flow rates caused burrowing into the ANFO.

Recommendations for angled blastholes are: the ANFO should be loaded as quickly as possible, then an initial smaller volume of stemming should be loaded slowly, after which it may be stemmed as desired.

## ***ACKNOWLEDGEMENTS***

The author would like to thank his principal advisor, Dr. Paul Worsey, for his guidance (and patience) during the completion of this thesis, and his committee members, Dr. John Wilson and Dr. David Barr, for their valuable input (and their willingness to read the whole thing).

More personally, the author would like to thank his family for their continued love and support during this educational venture. (The author would never forget to thank his family, because, of course, he still hopes that they do not remember how much he owes them).

Hopefully leaving no one out, the author would also like to thank the following people: the staff of Rock Mechanics for putting up with him; Ron and Jimmy at the UMR Experimental Mine for not only fixing the mechanical problems encountered during the research, but also taking the time to teach the author how to fix it next time it breaks; the summer crew at the Kappa Sigma Fraternity house for the vast hours of constructive slacking; all the brothers of the Beta Chi Chapter of Kappa Sigma for the repeated 'Are you still here?' comments which provided the needed motivation which the summer crew had drained from the author; the regulars at the Grotto for helping the author perfect his billiards and dart throwing ability; and last, but not least, the innumerable trees that gave their lives during the multiple drafts of this thesis.

## **TABLE OF CONTENTS**

	<b>Page</b>
ABSTRACT .....	iii
ACKNOWLEDGEMENTS .....	iv
LIST OF ILLUSTRATIONS .....	vii
LIST OF TABLES .....	ix
<b>SECTION</b>	
I. INTRODUCTION .....	1
II. THE PROBLEM .....	3
III. PREVIOUS WORK .....	5
A. OVERVIEW .....	5
B. STEMMING .....	5
C. ANFO: A WIDELY USED BLASTING AGENT .....	7
D. ADVANTAGES OF INCLINED HOLES .....	8
E. SUMMARY .....	10
IV. THE METHOD .....	11
A. OVERVIEW .....	11
B. DETAILED DESCRIPTIONS OF TESTING PROCEDURES .....	12
C. SUMMARY .....	23
V. RESULTS AND DISCUSSION .....	24
A. INITIAL ANFO ANGLE TESTS -- NO LOADING CHARACTERISTICS CONTROLLED .....	24

	<b>Page</b>
B. LOADING OF ANFO -- CONTROLLED FLOW RATES .....	25
C. MECHANISMS OF FLOW .....	28
D. INITIAL STEMMING RESULTS .....	31
E. TESTING WITH DIFFERENT TYPES OF STEMMING .....	35
F. HIGH-SPEED VIDEO RESULTS .....	39
G. ANALYSIS OF ALL TESTS .....	40
H. RESULTS DUE TO MODIFICATIONS IN TESTING .....	42
VI. THEORETICAL CONSIDERATIONS .....	45
A. PENETRATION POTENTIAL .....	45
B. POTENTIAL COMPLICATIONS ARISING FROM A NON-IDEAL INTERFACE .....	46
VII. CONCLUSIONS .....	50
VIII. RECOMMENDATIONS .....	52
IX. FURTHER STUDIES .....	53
APPENDIX A -- RESULTS OF EACH TEST SERIES .....	54
APPENDIX B -- VIDEO TRACINGS OF ALL TESTS .....	66
APPENDIX C -- FLOW RATE EQUATIONS AND SPREADSHEETS .....	72
APPENDIX D -- BULK DENSITY AND SIEVE ANALYSIS .....	76
REFERENCES .....	79
VITA .....	81

## LIST OF ILLUSTRATIONS

<b>Figures</b>	<b>Page</b>
I-1 Vertical vs. Inclined Bench Design (after Konya and Walter – modified) .....	1
IV-1 Illustration of Apparatus .....	13
IV-2 Photograph of Apparatus .....	14
IV-3 Design and Photograph of Flow Control Devices .....	16
IV-4 Eastman Kodak Spin Physics SP2000 .....	21
V-1 Plot of ANFO Loading Tests 1-10 .....	25
V-2 Typical ANFO/Air Interface Showing the Measure of the Angle of Deviation from Perpendicular .....	26
V-3 Analysis of Tests 11-49 .....	26
V-4 Typical ANFO/Air Interface Showing Unfilled Lengths of the Tube .....	27
V-5 Mechanics of Flow for Tests 11-49 .....	29
V-6 Secondary Analysis of Tests 11-49 .....	30
V-7 ANFO/Stemming Interface Progression .....	32
V-8 ANFO/Air vs. ANFO/Stemming Interface Tracings from Video -- S and N Series of Tests .....	34
V-9 ANFO/Air vs. ANFO/Stemming Interface Tracings from Video -- G, P, and DC Series of Tests .....	37
V-10 Video Images of Stemming Tests .....	38
V-11 Tracings of High-Speed Video Tests .....	40

<b>Figures</b>	<b>Page</b>
V-12 Analysis of All Stemming Tests .....	41
V-13 Tracings of the Modified Tests .....	44
VI-1 Pictorial Representation of Theoretical Stemming Problem .....	48



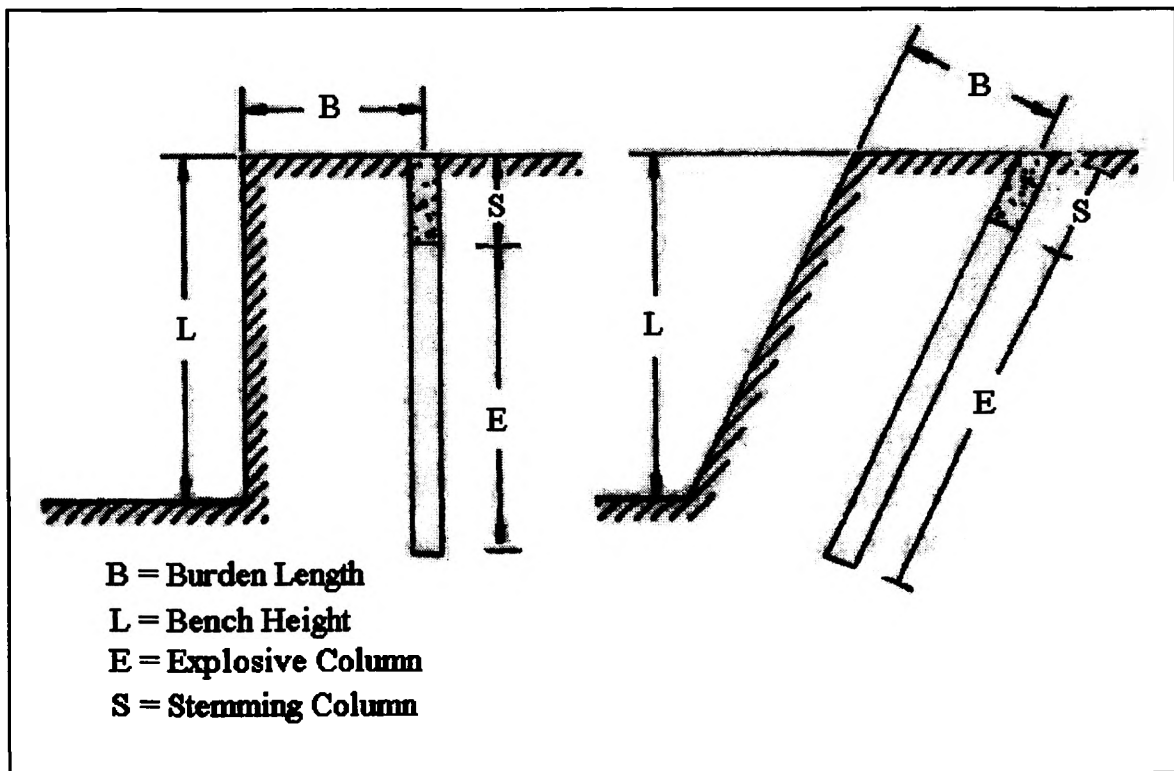
## LIST OF TABLES

<b>Tables</b>	<b>Page</b>
I -- Unfilled Lengths in 1-7/8's in. Tube .....	28
II -- Bulk Densities of Materials Tested .....	35
A-I -- Descriptions of Test Series .....	55
A-II -- Results of Tests 1-26 .....	56
A-III -- Results of Tests 27-49 .....	57
A-IV -- Results of Tests 1S-13S .....	58
A-V -- Results of Tests 14S-28S .....	59
A-VI -- Results of Tests 1N-16N .....	60
A-VII -- Results of Tests 17N-32N .....	61
A-VIII -- Results of Tests 33N-48N .....	62
A-IX -- Results of Tests 1G-16G .....	63
A-X -- Results of Tests 17G and 1P-12P .....	64
A-XI -- Results of Tests 1DC-12DC .....	65
B-I -- Video Tracings of S- Series Tests .....	67
B-II -- Video Tracings of N- Series Tests .....	68
B-III -- Video Tracings of G- Series Tests .....	69
B-IV -- Video Tracings of P- Series Tests .....	70
B-V -- Video Tracings of DC- Series Tests .....	71

<b>Tables</b>	<b>Page</b>
C-I -- Calculated Flow Rates of Each Material .....	73
C-II -- Calculations for Diameter Volumes per Second .....	75
D-I -- Bulk Density Calculations of All Materials .....	77
D-II -- Sieve Analysis of Drill Cuttings .....	78

## I. INTRODUCTION

The objective of blasting in the mining, construction, or demolition industries is to obtain the required result with the least amount of explosives. In mining, the object is to transfer as much as possible of the explosive energy into the rock that is being blasted. A blast hole must be drilled to allow the explosive charge to be placed in the rock for most efficient positioning. The problem is that the hole itself is the path of least resistance for the escape of the explosive energy after detonation of the explosive charge. To solve this problem, stemming is used to seal the hole. Figure I-1 illustrates a typical arrangement of a bench blast design in a surface mine.



**Figure I-1 -- Vertical vs. Inclined Bench Design  
(after Konya and Walter –modified).**

Stemming can be defined as any inert material placed on top of an explosive column for the purpose of sealing the blast hole and retaining the explosive energy within the ground. With a proper seal, the explosive energy will be confined, leaving the free face as the best means of rock movement. This provides the useful work as the rock between the blast hole and the free face is fractured and fragmented by the charge.

Surprisingly, there has been little in-depth work published on stemming as compared to other areas in explosives engineering. This makes the subject ideal for research. Blasting today still incorporates the use of 'rules of thumb' for suggested stemming practices. Research in the past has helped to narrow the range of some of these 'rules', but the interaction between the explosive and stemming during the stemming process has been generally overlooked.

It is normally assumed that when granular explosives such as ANFO are poured into a vertical blast hole, the final surface of the mass will be flat and horizontal, perpendicular to the walls of the blast hole. It is also assumed that any stemming material poured onto this ANFO surface will result in an interface that is similarly flat and horizontal. This may be a valid assumption, but once the angle of the blast hole deviates from vertical, little is known as to the nature of the interface.

The purpose of this research is to investigate what happens during the loading and stemming of angled, non-vertical holes. This will help to develop a model for the mechanisms involved and to determine stemming recommendations where necessary.

## ***II. THE PROBLEM***

Studies of the stemming process cannot be implemented in the field because the blast holes are located in the ground. Since earth materials are generally opaque, the actual mechanisms involved during the stemming process cannot be viewed. It is clear that to study the dynamics of a blast hole, a laboratory simulant of a blast hole must be used.

Once a proper simulant for a blast hole is created, various tests can be performed. The questions that this research seeks to answer about angled holes are as follows:

- What does the interface between the ANFO and the stemming look like?
- Is the interface clearly defined or does mixing occur?
- What are the factors that control each interface?

The ideal interface for maximum efficiency of both the explosive and the stemming would be a flat surface, perpendicular to the walls of the blast hole. This type of interface is that which is assumed during the design of the blast hole. The design of the blast hole includes, among other things, the length of the explosive column and the length of the stemming column (See Figure I-1). If the interface between the explosive and the stemming is not flat, then the field lengths will not match the design lengths. Complex interfaces may include mixing which will introduce dilution of the explosives or may affect the performance of the stemming material.

A flat perpendicular surface can readily be attained in a vertical hole, but not much is known about what types of interfaces occur in angled holes. To answer these

questions, extensive testing was conducted at the University of Missouri-Rolla Experimental Mine and the Rock Mechanics and Explosives Research Center as described in Section IV: *The Method*.

### ***III. PREVIOUS WORK***

#### ***A. OVERVIEW***

The breadth of publications on stemming research in the past has generally been limited in scope to how much stemming is necessary and what size range is ideal. Not much has been published on the processes that occur during stemming or those involving the interactions of the explosive and the stemming. This section will document previous research and published recommended practices. In addition, materials will be discussed in areas supporting certain choices made in this thesis including the use of ANFO as the preferred blasting agent, and the advantages of using angled blast holes.

#### ***B. STEMMING***

Stemming can be defined as an inert substance loaded on top of the explosive column, which provides confinement for the explosive energy (Atlas Powder Company, 1987). Studies show that a high explosive charge needs to be confined in order to function properly and release the maximum energy (Konya and Walter, 1990). Proper confinement, however, is a factor of the performance of the stemming which is dependent upon of the length of the stemming column and the average size of the particles making up the stemming.

The length of the stemming column is a critical factor. There is a delicate balance between insufficient stemming and excessive stemming (Atlas, 1987). When insufficient stemming is used, there is the possibility of premature ejection from the hole which leads in many cases to excessive flyrock and airblast. When too much stemming is used, it

may cause excessive ground vibrations and can create large boulders in the muck pile, which are derived from the unloaded portion of the hole.

There are tested guidelines for the proper length of stemming, but all recent research points out that with changing rock conditions, the optimum amount of stemming may vary from the suggested lengths. In fact, the establishment of suggested lengths of stemming is a fairly recent development. In the sixties, it was still common to leave 0.5 to 1 times the length of the burden unloaded and empty, or sometimes stemmed with dry sand (where the burden length here is the distance between the rock face and the blasthole) (Langefors and Kihlström, 1963). In the late 80's, many different suggestions were given for proper stemming length. Konya and Walter, 85 suggested a length of 0.7 times the burden, while Olofsson, 88 suggested that the stemming length should be equal to the burden length. Others took a broader approach and proposed a proper stemming range between 0.7 and 1.3 times the burden (Atlas, 1987). Alternative research using mechanical stemming plugs have effectively reduced the required stemming amount by a range between 1/2 and 1/3 that of a non-plugged stemming column (Worsey, 1988, 1990). However, one common factor emerging from all of these publications is the fact that too much or too little stemming can cause problems. With this delicate balance in mind, it is necessary for the designers of a blast to know that the lengths of the explosive and stemming columns are accurate for a given design of shot. Therefore, if excessive flyrock or boulders occur, appropriate changes to the design can be implemented.

The size of stemming is important to properly seal the blasthole. Stemming should lock into the borehole walls when the blast pressures are exerted onto it (Konya



and Walter, 1990). Drill fines or rock dusts are still commonly used, but should be avoided since they do not lock into the blasthole walls and are easily ejected from the hole. This is especially true with some of the drill fines produced by today's percussive hydraulic impact drills.

Atlas Powder Company guidelines to stemming sizes are given below.

Hole Diameter (in.)	Average Stemming Size (in.)
1-1/2	3/8 – minus
2 to 3-1/2	3/8 to 1/2
4 to 5	5/8
5 and up	3/4 – minus

Konya and Walter, 90 have proposed a simple formula for stemming sizes. They state that the average stemming size should be 0.05 that of the hole diameter. This is analogous to dividing the hole diameter by 20. This equation results in a much smaller stemming range than that which Atlas recommends. Fitting the Atlas chart to a similar equation would result in the stemming size being roughly equal to the hole diameter divided by 8. For the purposes of this research, anywhere within the range of these two recommendations was deemed adequate since this follows within industry standards.

### **C. ANFO: A WIDELY USED BLASTING AGENT**

ANFO, or Ammonium Nitrate and Fuel Oil, was the explosive chosen for this research because it is used more frequently in blasting operations than any other explosive. Since the 50's when ammonium nitrate (AN) first saw its use in blasting agent production, the use of ANFO type products has greatly increased. ANFO production has increased from a few thousand pounds in 1955 to over 2.2 billion pounds in 1974 (Dupont, 1977). The latest Explosive Consumption Survey has shown that over 5 billion

pounds of explosives were used in 1995, of which approximately 85% consisted of ANFO type products (USBM, 1995). The reason for the popularity of ANFO is that it is the most economical of today's explosives. The only major drawback to ANFO is that it is not a waterproof explosive, so special liners must be used if it is to be implemented in wet conditions (Leader, 1981), (Rossow, 1985). Still, with the widespread use of ANFO, it is clearly the best target for research considerations.

#### **D. ADVANTAGES OF INCLINED HOLES**

The use of inclined holes in blasting practice, i.e. angles deviated from vertical, has increased in the recent past. This increase is due to numerous advantages of the system, and the emergence of new technologies that deal with the disadvantages.

Inclined holes are commonly used in the following applications:

- Blast Casting (Chiappetta, et. al, 1990), (Rollins and Givens, 1988)
- Cut Slopes on Highways and Other Civil Works (Worsey, 1981)
- Slope Stabilization (Stachura and Cumerlato, 1995),
- Mining in Unfavorable Ground Conditions (O'Meara, 1994),  
(Trudinger, 1973)

There are several advantages to using inclined holes in these applications:

- Inclined blast holes paralleling the free face use blast energy more effectively.
- Greater reflected energy results in more efficient fragmentation of the rock.
- The loading factor may be reduced due to reduced resistance at the toe.
- The angle of breakage at the bottom of the hole is greater, making it easier to break and loosen the rock.
- Muck piles can be excavated more easily because of more freedom of movement.

(Army Corp of Engineers, 1972)

Furthermore, it has been shown that increasing the amount of powder in an inclined hole can displace or throw a percentage of the overburden to the spoil pile. This is called blast casting. Blast casting has the potential for considerable savings since it reduces the amount of overburden stripping necessary (Dupree, 1986). The ideal angle for blast casting would be on a 45 degree from vertical trajectory, but due to the increased cost of loading holes at these angles, the majority of casting operations in the U.S. use casting angles of about 20 degrees from vertical. Casting angles are rarely over 30 degrees from vertical due to economic limitations (Brown, 1997).

Another major advantage of inclined blast holes is that the resulting slope after a blast is more stable due to the lowered angle. Coupled with this is the fact that inclining the blast hole results in a reduction of back break and unwanted fracturing of the remaining highwall. In a vertical hole, the explosive charge tends to fracture at a naturally dictated angle called the 'back break angle'. This phenomenon can cause instability in the highwall resulting in an excessive amount of rock leftover at the toe of the slope that can cause severe problems in subsequent blast design. The true estimate of back break in an inclined hole, however, is the back break angle minus the hole angle. This reduction in the true back break angle reduces the amount of toe, which in turn improves diggibility (Favreau, et. al, 1988).

The main disadvantages of inclined drilling includes the fact that it is more difficult to align the holes correctly due to improper drilling practices, and drill bit wear is increased. Misalignment of the holes may result in excessive flyrock or large boulders that have to be secondary blasted. Yet, with recent advances in the technology of laser

profiling, borehole deviation measurements, and computer modeling of the rock face, these concerns and other hazards have been reduced or eliminated (O'Meara, 1994).

### ***E. SUMMARY***

The actual loading processes that occur while stemming a blasthole have not been thoroughly researched in the past. While researchers agree that the appropriate length and size of stemming is necessary for the most efficient blast, not all can agree upon the same values of 'appropriate'. With this in mind, it was the goal of the research in this thesis to study the loading process of stemming as an integral variable in stemming performance. The work in this thesis has concentrated on the loading processes of commonly used inclined blastholes charged with ANFO.

## ***IV. THE METHOD***

### ***A. OVERVIEW***

The approach used in this research was to simulate the loading and stemming of a blast hole in a repeatable fashion. To realistically simulate these processes, all tests were performed without the loader being aware of what was happening in the blast hole so that visual stimuli did not affect the actions of the loader.

A video camera was used to record all data as the loading processes were carried out. This data was used as a supplement to the visual data acquired after each test for later analysis. The visual data consisted of angle and displacement measurements where possible, plus a sketch and brief description of the final interface. The video camera data allowed for in-process descriptions as well as before and after interface sketches.

The testing in this research project entailed the following steps:

- The fabrication of a blasthole simulant for testing.
- The design of Flow Control Devices after the initial testing of the ANFO/Air interface concluded that the flow rate of the material was a major variable.
- Small-scale testing of the ANFO/Air interface using the flow control devices. This testing led to an analysis of the flow mechanics evident during ANFO loading.
- Small-scale testing of the ANFO/Stemming interface using sand as the stemming agent.
- The expansion of scale to test the effects of larger diameters on the ANFO/Stemming interface.
- The substitution of different stemming materials including gravel, pea gravel, and drill cuttings to test particle size and density effects on the ANFO/Stemming interface.

- High-speed video analysis of the material interactions evident during the stemming process.
- Developing and testing of the best theoretically developed method for loading.

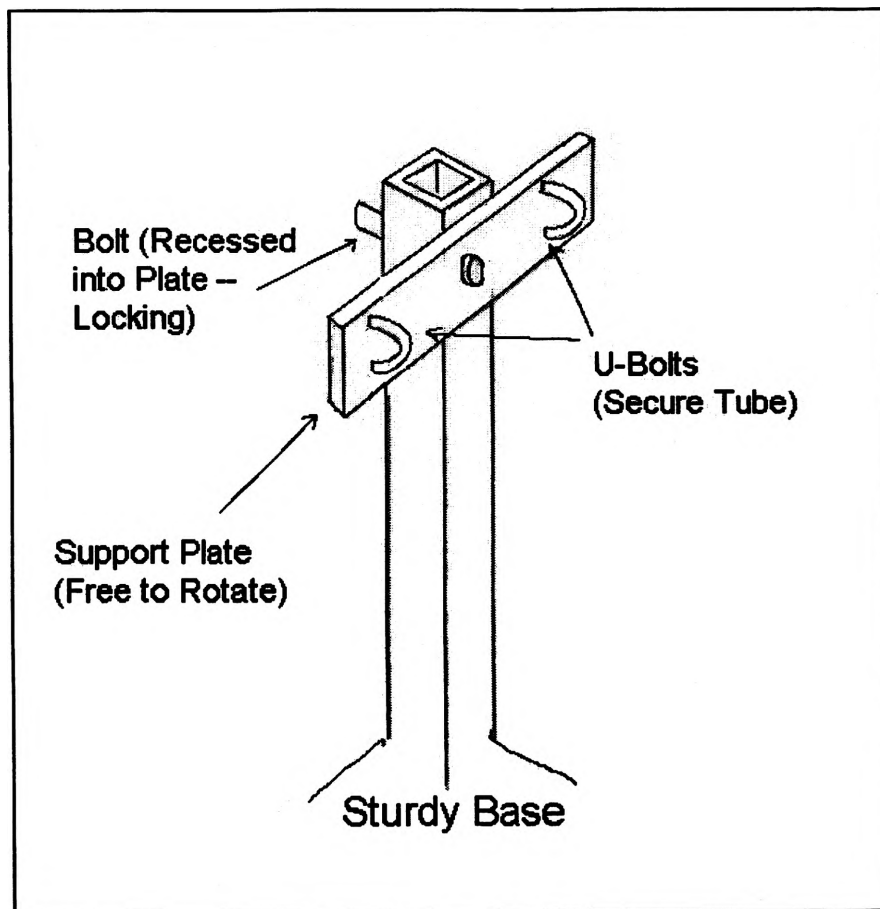
The outlined procedure is described in detail in the following subsection. Individual data sheets for each array of tests can be found in Appendix A.

## **B. DETAILED DESCRIPTIONS OF TESTING PROCEDURES**

1. Creating a suitable simulation of a blast hole was the first step. Since rock is generally opaque and translucent at best, clear plastic tubes were chosen as the desired simulant. It was advantageous to use the plastic tubes mainly because of their transparent nature, but also because of their low cost and good availability. It was evident that the surface of the plastic was not exactly comparable to borehole conditions, but since the study was concentrating on the ANFO to stemming interactions and not the material to wall interactions, this discrepancy was not deemed critical. In fact, high-speed video of the tests showed that most of the material rode on a small air cushion, and was not in complete contact with the tube walls. This helped confirm the suitability of the plastic simulant.

For thoroughness, three tube sizes were selected that had internal diameters of 1-7/8, 3, and 4-1/2 inches. These diameters were considered small enough to simplify testing, but were also comparable to actual blast hole sizes used in industry (Section III: *Previous Work*).

A durable apparatus was constructed to secure the tubes as illustrated in Figure IV-1. The apparatus was made of a fixed upright steel beam to which a rotating plate was attached that could be locked to the beam at any angle desired by using a long bolt. The clear tubes were attached to the plate, and an adjustable angle level was taped to the tube for setting the required angle. The apparatus was built stable enough to retain a constant angle even under dynamic loading conditions. A photograph of the apparatus is shown in Figure IV-2.



**Figure IV-1 -- Illustration of Apparatus.**



**Figure IV-2 -- Photograph of Apparatus.**



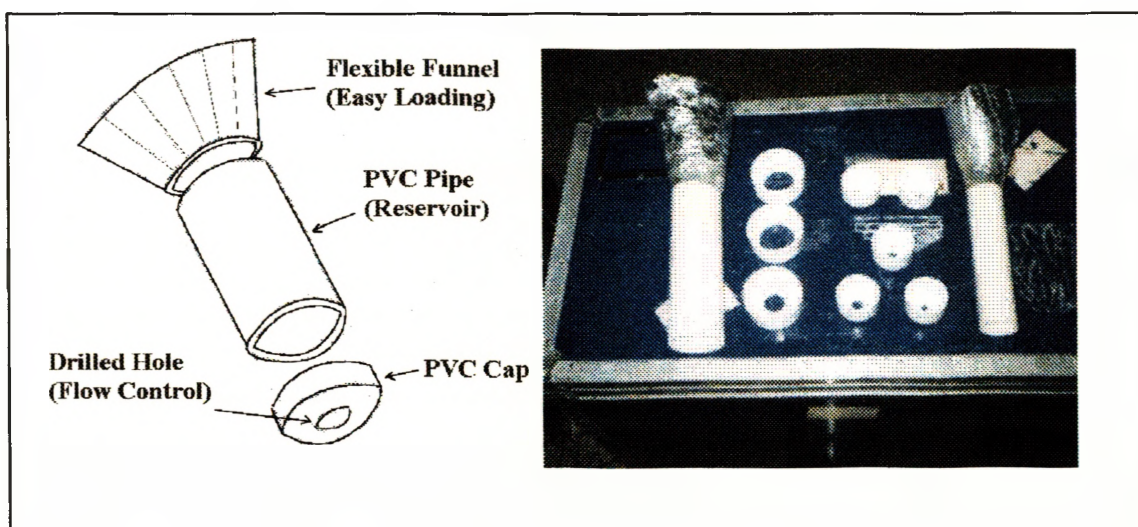
2. The initial tests were designed for the purpose of determining how ANFO behaves during the loading process alone. The tests consisted of pouring ANFO into the 1-7/8 in. tube starting at a vertical angle. In successive tests the angle was inclined away from vertical until the ANFO would no longer flow into the tube. In each test, the ANFO was poured from a bucket container into a funnel that was connected to the tube.

After only ten tests, it was quickly determined through video playback that the flow rate of the ANFO was an important factor that controlled the final angle of repose, the degree of curvature of the ANFO/Air interface, and the loading mechanism involved. For this reason, testing procedures were modified to control flow rates as described in the next subsection.

3. To control the flow rates of the materials during further testing, and to determine the effect of these different flow rates on the ANFO/Air interface, specialized loading devices were constructed. These devices consisted of PVC pipes and caps with different size holes drilled into the caps. The PVC pipe was used as a storage volume for the material to be used in each test. The drilled caps were used as nozzles to control the flow rates of the material pouring out of the PVC pipes. Smaller drill holes in the caps meant slower flow rates of material, while larger drill holes meant faster flow rates of material.

The process of loading during each test was completed in several small steps. First, a PVC pipe was chosen that was near the size of the blasthole to be tested to provide ample material in the PVC reservoir. For this research, only 2 and 3 in. pipes were necessary. Once the pipe was chosen, a predrilled cap was fitted to the end of the pipe. Next, the operator's hand was used to close off the hole while ANFO or stemming,

depending upon the test, was loaded into the pipe. Finally, upon quick release of the operator's hand, the material would leave the PVC reservoir at a flow rate dictated by the diameter of the drilled hole. Figure IV-3 shows the design and a picture of the flow control devices.



**Figure IV-3 – Design and Photograph of Flow Control Devices.**

The flow rates of each nozzle were calculated using marked lines of known volumes on the clear plastic tubes of the apparatus shown in Figure IV-2, and with the use of a stopwatch. Recording the time between marks allowed for calculation of the loading rates. These flow rates were initially calculated in mL/s.

For purposes of scaling the experimental hole diameters to larger diameters, the flow rates were converted to units of diameter volumes per second, where a diameter volume is the volume representing the area of the hole times a length equal to the diameter. The equation for a diameter volume is as follows:

$$1 \text{ DV} = (\pi * d^2 / 4) * d \quad \text{or} \quad \pi * d^3 / 4$$

where:  $DV = \text{diameter volume, cm}^3, \text{ mL}$

$d = \text{diameter, cm}$

The equation to convert the flow rate in mL/s to diameter volumes per second is as follows:

$$DV / s = (FR) / (DV)$$

*where: FR = Flow Rate in mL / s*

*DV = diameter volume for blasthole, mL*

Calculating flow rates in this manner allows the results to be scaled to any diameter of blast hole. For example, a value of 2 DV/s for sand in the 1-7/8 in. tube equates to 173.5 mL/s while 2 DV/s for sand in the 3 in. tube equates to 702.2 mL/s. This scaling effect takes into account the relative volumetric differences of the larger tubes.

Flow rates of every material were measured in this manner for the nozzle sizes used in the tests. The size distribution and density of each material altered flow rates even for the same diameter nozzle, so each material had to be tested independently. Also, it was necessary to determine the relative bulk density of each material at this time (Appendix D).

4. Tests were then continued using five known flow rates of ANFO for each angle tested previously, that is vertical then decreasing till the tube no longer filled. With a constant rate of flow, the ANFO/Air interface was flat, and its angle relative to perpendicular to the length of the tube could be easily measured. Failure to completely fill the hole occurred around 55 degrees from vertical, and no filling at all was evident beyond 65 degrees from vertical. For this reason, the natural angle of repose of the

ANFO was measured to see if there was a correlation. A total of 39 tests were performed to investigate this aspect of the experimentation.

5. From video recordings of all the previous tests, the mechanisms of flow were observed at each angle and flow rate. The observations included the prill to prill interactions of the ANFO such as avalanching, burrowing, grain size sorting and radial displacement.

6. With the mechanics of the ANFO loading fairly well understood, testing proceeded to the interaction of the stemming and the explosive column. A typical test comprised loading the 1-7/8 in. tube with ANFO at a fixed flow rate, then adding stemming at a fixed flow rate. The initial stemming used was medium sized filter sand (minus 1/8 inch) that was obtained locally. After each test, the tube was emptied, and the sand was separated from the ANFO by means of a #14 Tyler series sieve for minimization of waste.

The range of tests denoted 1S-28S involved two flow rates of ANFO (0.7 and 12.6 DV/s), with six flow rates of stemming (0.35, 0.64, 1.14, 1.58, 2.05, and 12.85 DV/s), for angles spaced 10° apart ranging from 40° to 80°. The angle of the ANFO/Air interface was measured each time before loading the stemming material to help measure the overall change to the ANFO/Stemming interface. After the stemming was added, a description of the resulting interface was recorded, and an angle or depth of burrow was measured where possible. A total of 28 tests were performed at this stage, plus 14 repeats to determine the repeatability and validity of the results. The repeated tests mentioned

here and later in the text describe ANFO loading tests only. These tests were necessary since each test in the stemming series required the loading of ANFO then stemming, so it was essentially two tests in one. The amount of repeated tests depended entirely upon the specified parameters of each set of testing.

7. From the previous tests, it was evident that the stemming material was burrowing into the ANFO, even at angles close to vertical. For this reason, the scope of the research changed to concentrate on the more practical angles that are used in industry, such as in the blast casting application (Section III: *Previous Work*). Since blast casting utilizes angles from nearly vertical to rarely more than 30 degrees from vertical (60 degrees from horizontal), the next set of tests were narrowed to the following angles: 10, 20, and 30 degrees from vertical.

For completeness in testing and to provide data to confirm the reliability of using diameter volumes for scaling effects, it was decided to use larger tube sizes namely 3 in. and 4.5 in. tubes. Testing continued with the 3 in. diameter tube with sand as the stemming agent. An extensive series of 50 tests were performed with 44 ANFO loading test repeats. Testing parameters for test series 1N-50N included three angles (60°, 70°, 80°), three ANFO loading rates (1.19, 3.79, and 7.19 DV/s), and four stemming rates (0.80, 3.14, 3.18, and 5.27 DV/s).

From these tests, it was noted that the original ANFO/Air interface had minimal bearing on the final ANFO/Stemming interface. The flow rate of the stemming and the angle of the tube were the primary factors. This permitted the number of future tests to be reduced by using only the high and low flow rates for the ANFO.

8. The next set of tests were carried out using the 3 in. tube, however, the stemming was changed to 1/8 - 1/4 in. gravel. The purpose of these tests was to show the different effects, if any, of different stemming materials. The testing parameters for test series 1G-15G included three angles ( $60^\circ$ ,  $70^\circ$ , and  $80^\circ$ ), two ANFO loading rates (high and low), and three stemming rates (2.53, 1.69, and 2.56). Two of the stemming rates were found to be nearly equal. This coincidence was caused due to the change from the 2 in. PVC pipe to the 3 in. PVC pipe in the flow control device. However, the similarity of the results of these tests provided verification of the repeatability of the process. There were 15 tests performed plus 15 repeats. A record of all results was taken in the same manner as mentioned and described previously in subsection 6.

9. High-speed video was used to determine the exact nature of the burrowing process that was viewed in the tests previously recorded by regular 8mm video. A total of 6 tests were performed using an Eastman Kodak Spin Physics SP2000 high-speed video camera (Figure IV-4) set to 500 frames per second. The tests incorporated sand and gravel as the stemming materials at three different flow rates (1.69, 2.53, and 3.14) for two different angles ( $60^\circ$  and  $80^\circ$ ).



**Figure IV-4 -- Eastman Kodak Spin Physics SP2000.**

10. For the 4.5 in. tube, larger stemming was necessary to more accurately simulate a loaded blast hole as used in industry. Pea gravel was chosen with a size range of 1/4 to 3/4 in. (See Section III: *Previous Work*). Testing parameters for test series 1P-9P included three angles (60°, 70°, and 80°), one ANFO loading rate, and three stemming rates (0.45, 0.86, and 2.24 DV/s). There were 9 tests performed plus 6 repeats. The record of all results was taken the same as previously described in subsection 6.

11. For completeness, one set of stemming tests used drill cuttings obtained from the field for the stemming material. The cuttings were collected from Capital Quarries just north of Rolla, Missouri. The cuttings derived from a Furukama HCR15-ED hydraulic drill that was used to drill 3.5 in. holes. A sieve analysis was performed on the cuttings and the results can be found in Appendix D. The 3 in. tube was used because it was the closest to the actual hole diameter that the cuttings were removed from. The testing parameters for test series 1DC-9DC included three angles ( $60^\circ$ ,  $70^\circ$ , and  $80^\circ$ ), one ANFO loading rate, and three stemming rates (1.05, 2.02, and 3.23 DV/s). A total of 9 tests were performed plus 9 repeats. A record of the results was performed in the same manner as previously described in subsection 6.

12. Throughout the testing, it became evident that a slower rate of stemming flow did not burrow as deeply into the ANFO as a faster rate of stemming flow. However, since the speed of loading is important in most mining applications, loading the entire stemming column slowly would undoubtedly cost more money than the problems created by fast loading. For this reason, it was rationalized that if a small portion of the stemming was loaded slowly, then the rest of the stemming column could be loaded at any rate and not affect the interface. This theory was partially developed during previous sand stemming tests in which a clump of sand was accidentally released before the main mass (Tests 35N, 39N, 45N, and 47N). The results of these tests showed the least disturbed interfaces, so a series of tests were designed for each stemming material to collect data on this theory. A selection of 9 of the tests included stemming a small amount at substantially lower flow rates before the bulk of the stemming was added at the



fastest practical flow rate. There were three tests completed for each type of stemming material (16G-18G, 10P-12P, and 10DC-12DC), i.e. one test for each angle (60°, 70°, and 80°).

The main objective of these tests was to find out the volume necessary in the initial clump of stemming. Most of the data, therefore, was collected using the video recordings of each test. These tests enabled the best ANFO/Stemming interfaces of all the tests, and provided support for the final recommendations of this research.

### **C. SUMMARY**

A total of 277 recorded tests were performed during the course of this research at the University of Missouri-Rolla. A breakdown of the types of tests follows:

• ANFO loading tests	49
• Repeated ANFO loading tests	88
• Stemming Tests	129
• High-Speed Video Tests	6
• Density Measurements	5
Total	277

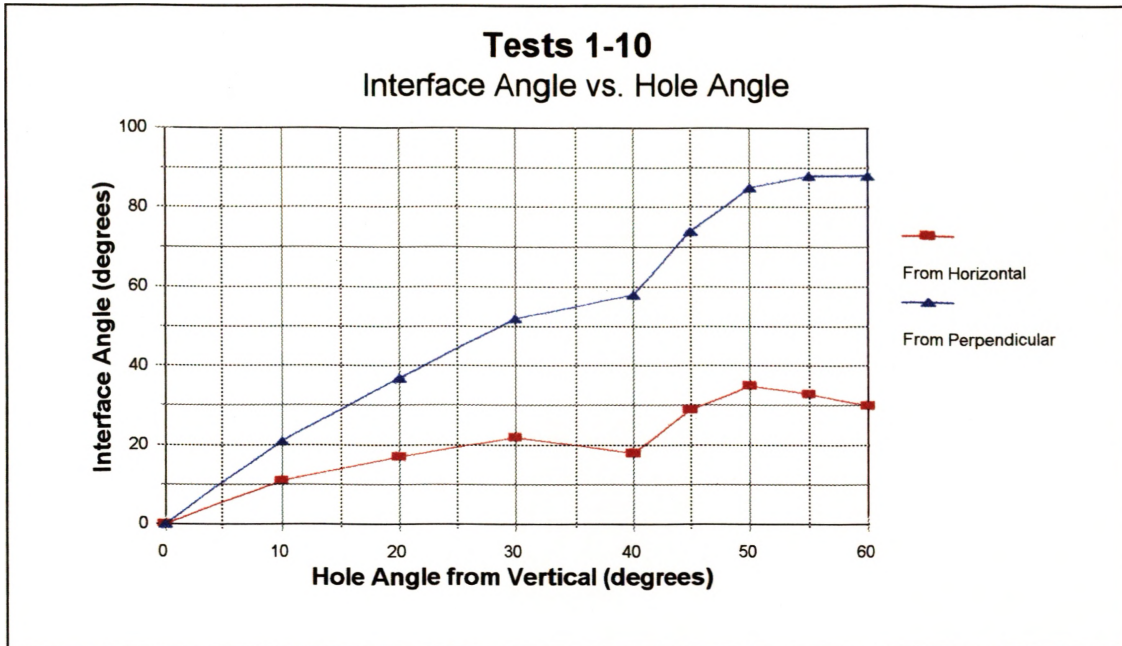
## ***V. RESULTS AND DISCUSSION***

Since this research involved the interaction of granular materials during the stemming process of loading a blast hole, it was not known what types of interactions would occur, or how complex of an interface would be created. As it turned out, there were varying degrees of complexity that made quantitative numerical descriptions of the results difficult. For this reason, sketches and descriptions were taken for all tests, and actual numerical values of angles and distances were measured whenever possible. This approach has resulted in the presentation of the results of these tests to be a qualitative and quantitative mixture. Charts and graphs were constructed where possible, however, much of the data is presented in narrative form.

The tests conducted can be subdivided into several categories by reason of a fundamental change in the procedure. The results are subdivided according to the size of the hole used, the type of stemming used, and the type of test performed. The results follow the same sequential order as described in Section IV: *The Method*.

### **A. INITIAL ANFO ANGLE TESTS – NO LOADING CHARACTERISTICS CONTROLLED**

The initial ten tests were performed without control of the flow rate during loading. The results of these tests can be seen in Figure V-1. From the graph in Figure V-1, it was noted that the results showed considerable scatter instead of a smooth curve as expected. This suggested that other variables were in play and were affecting the results. As such, there was not sufficient control in the tests.



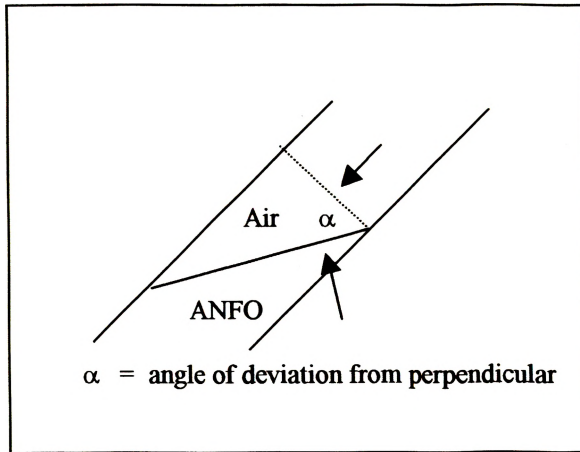
**Figure V-1 -- Plot of ANFO Loading Tests 1-10.**

From an analysis of the video recordings of these tests, it was evident that the angle of the wave front of the ANFO as it was poured into the tube was affected by the speed at which the material was poured. Also, the final surface of the ANFO/Air interface was complex and not flat as expected. It was noted that the flow rate of the last portion of material gave the resultant final angle. It was clear that to get accurate data, the flow rates of the materials had to be controlled.

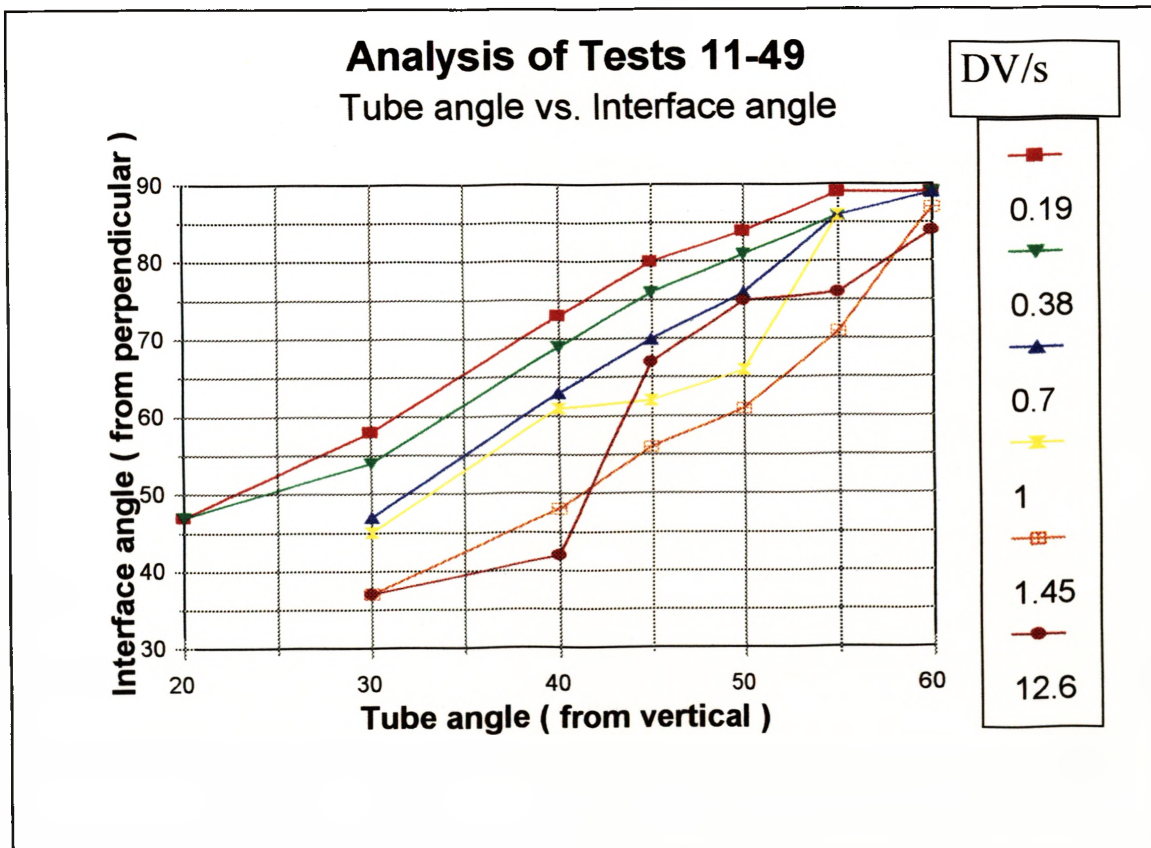
### **B. LOADING OF ANFO – CONTROLLED FLOW RATES**

Tests 11-49 were carried out using 6 different flow rates (0.19, 0.38, 0.7, 1.0, 1.45, and 12.6 DV/s). For each flow rate, the deviation of the interface angle from perpendicular to the tube (illustrated in Figure V-2) was plotted against the tube angle as

shown in Figure V-3. The raw data for these tests and the individual plotted curves are found in Appendix A.



**Figure V-2 -- Typical ANFO/Air Interface Showing the Measure of the Angle of Deviation from Perpendicular.**

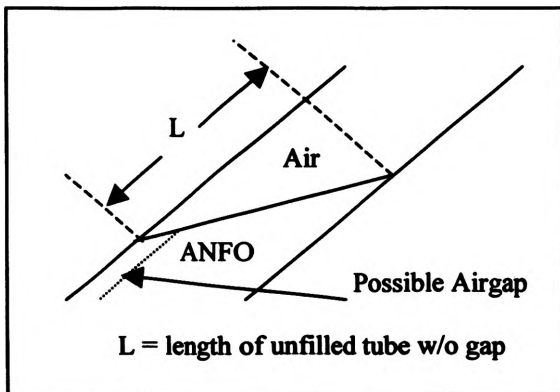


**Figure V-3 -- Analysis of Tests 11-49.**

From Figure V-3, it can be seen that there is a natural progression of deviation from perpendicular as the flow rate increases. Though there was some experimental aberration in the higher flow rates, in general, the higher the flow rate, the less the deviation angle. Subsequent repeated tests smoothed out the curves in Figure V-3, but the results remained the same.

It should be noted that the large increase from 1.45 DV/s to 12.6 DV/s did not affect the angles to any great extent. This is probably due to the approach of a cutoff angle dictated by gravity and the natural angle of repose of the ANFO.

The tests also showed the maximum hole angle that ANFO could be effectively loaded by gravity alone. As the angle of the tube increased and the ANFO/Air interface deviated from perpendicular, a certain length of the tube was not completely filled as illustrated in Figure V-4. At steeper angles, the tube would sometimes never fill completely, leaving an air gap along the back for the entire length of the tube. Table I shows the data for the length of the unfilled portion of the tube during tests 11-49.



**Figure V-4 -- Typical ANFO/Air Interface Showing Unfilled Lengths of the Tube.**

**Table I -- Unfilled Lengths in 1-7/8's in. Tube**

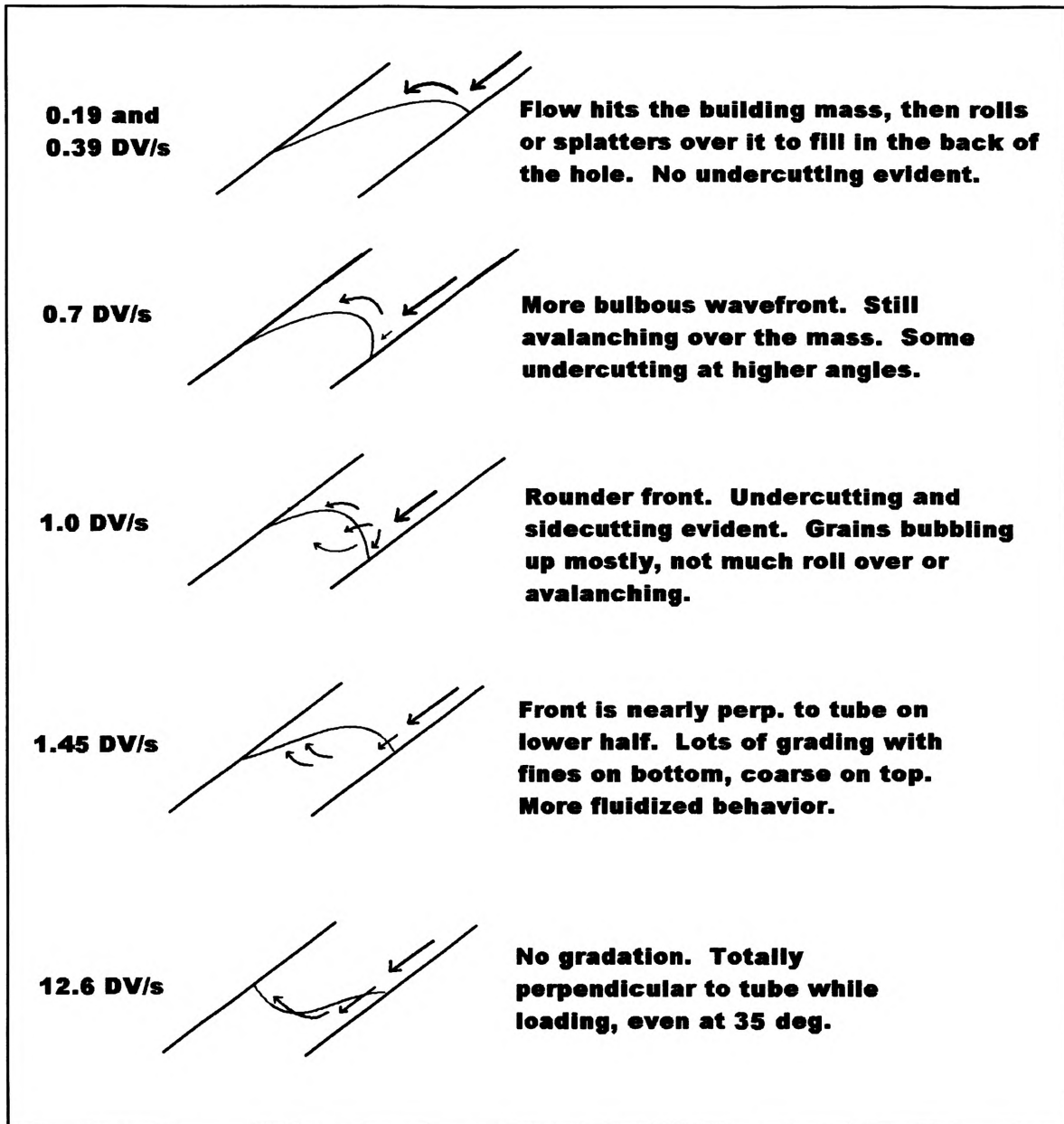
Tube Angle from vertical	Diameter Volumes per second (DV/s)					
	0.19	.038	0.7	1.0	1.45	12.6
20°		1.8				
30°		2	2.3	2	1.3	1.8
40°		3.5	3.3	3	2.3	2.3
45°	5.3	5.5	3.8	3.5	2.8	
50°	9.8	8.8	7.5	5.8	4.5	4.5
55°	X	40	60	X	X	6
60°	X	X	X		X	16.3

All values in inches. X = unfilled air gap for entire length of tube

Table I shows a natural cutoff for loading angled holes by gravity at 50° from vertical. Anything beyond 50° did not load properly. The angle of repose for ANFO was determined to be 58° from vertical which corresponds well with this natural cutoff. In fact, experiments showed that the ANFO would not even pour into the 65° hole, and piled up at the mouth of the tube.

### **C. MECHANISMS OF FLOW**

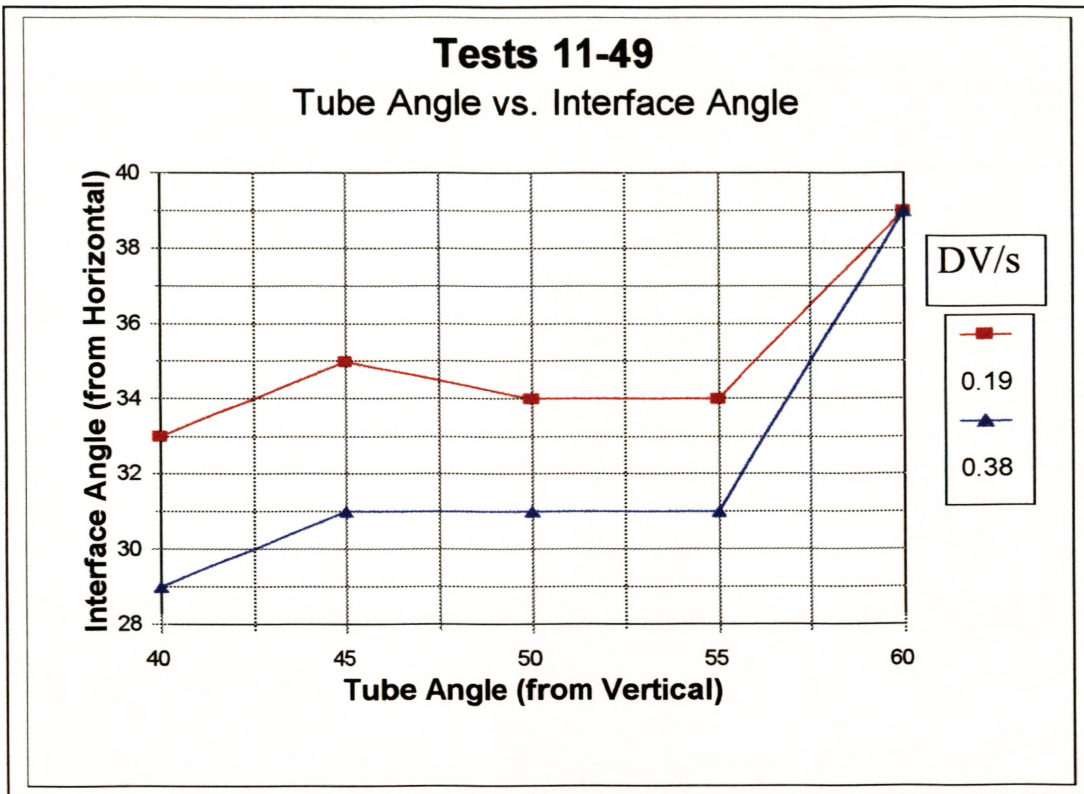
Video analysis of the first 49 tests showed that there are different processes involved when loading ANFO by gravity. Depending upon the flow rate, different mechanisms of flow seem to exist as the ANFO grains interact under varying loading conditions. Figure V-5 shows a pictorial and descriptive explanation for the different mechanisms of flow observed.



**Figure V-5 -- Mechanics of Flow for Tests 11-49.**

Figure V-5 shows that at lower flow rates there was not much penetrating power, so when the ANFO hit the building mass, it rolled over the top in an ‘avalanching’ process. In fact, from Figure V-2, if the angle of interface was found with respect to horizontal by subtracting out the tube angle (Figure V-6), then the two lower flow rates

consistently showed an angle near  $32^\circ$  ( $58^\circ$  from vertical), the calculated angle of repose for ANFO.



**Figure V-6 -- Secondary Analysis of Tests 11-49.**

As the flow rate increased, the deviation angle with respect to horizontal decreased, showing that different processes were at work as seen by the shifting curves in Figure V-3. At 0.7 and 1.0 DV/s the ANFO seemed to gain the penetration power necessary to undercut the building mass. This undercutting pushed the mass upward toward the back. Finally, at 12.6 DV/s, the sheer volume of the incoming mass filled the entire tube leaving no chance for intermixing of grains.

It is interesting to note the behavior of the ANFO when the undercutting process occurs. As the mass was lifted upwards, or bubbled up, a distinct gradation of the grains was formed with the coarse grains moving to the top and fine grains to the bottom.



#### **D. INITIAL STEMMING RESULTS**

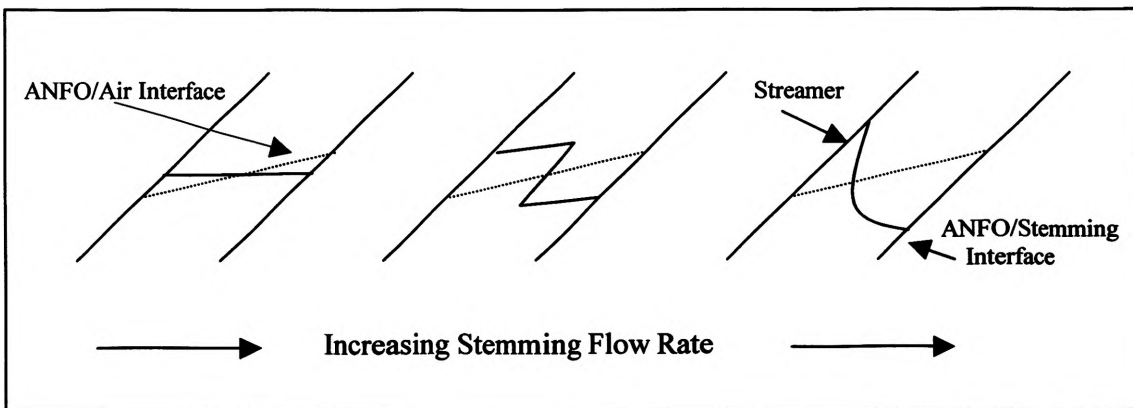
The results of tests 1S-28S show the first effects of the stemming process on the ANFO/Stemming interface. The stemming material used was medium sized sand that was oven-dried and then allowed to reabsorb moisture only from the atmosphere. The flow rate of the ANFO was limited to two flow rates for initial simplicity while the sand was poured at four different flow rates. A complete listing of all the data is presented in Appendix C.

The number of the ANFO flow rates were limited in these tests to enable data to be acquired quickly about the stemming only, so any changes to the procedure could be implemented if necessary. As it turned out, a good deal of information was recovered from these 28 tests, although this was not evident until all of the research tests were complete.

For the two different ANFO flow rates, 0.7 and 12.6 DV/s, there were striking similarities in the results for the faster flow rates of sand. Not only were the resulting interface angles comparable, but the complex interfaces were also similar. This led to the conclusion that the density of the ANFO, when compared to the sand was insignificant, and thus the sand flow rates alone would be the controlling factor in the final interface, not the initial ANFO/Air interface. To prove this, extensive testing was carried out in tests 1N-50N.

The 3 in. tube was used for tests 1N-50N. Also, three different ANFO rates were used with four different stemming rates (still sand). From these tests and from tests 1S-28S, the following correlation was found that was linked to the flow rate of the stemming. At lower flow rates, around 1 DV/s, the sand stemming seemed to push the

ANFO and then avalanche over itself in a similar fashion to the ANFO flow mechanics seen in the previous subsection. At higher flow rates, above 1 DV/s, the sand would burrow into the ANFO and throw the grains to the other side of the tube. Between these two phenomena, a combination of pushing and throwing occurred that formed a shape like a step. Figure V-7 shows an example of the progression of interfaces from low to higher flow rates of stemming.



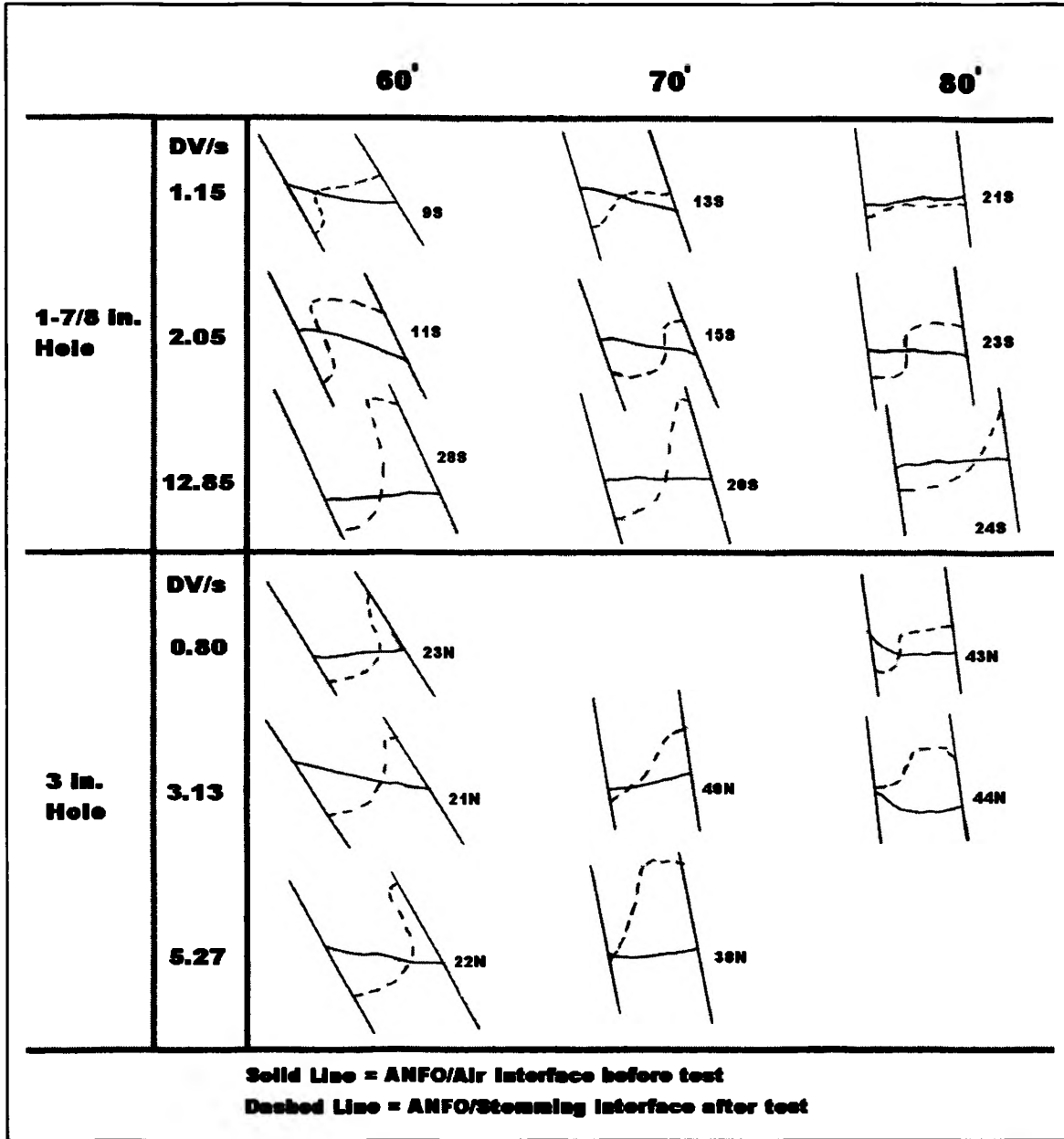
**Figure V-7 -- ANFO/Stemming Interface Progression.**

The higher flow rates of the stemming in these tests resulted in an interface resembling a crater impact. At times, the hanging wall side of the tube would have a streamer of ANFO greater than 2 in. in length as shown in Figure V-10. In some tests, the streamer extended the full length of the stemming column, leaving grains of ANFO on top of the stemming material. The main effect of this type of burrowing was to raise the explosives to a level higher than expected. Comparing a 2 in. throw in a 3 in. tube to a 15 in. tube could lead to explosives being 1 ft. higher than designed. Also, the complex step function evident in some tests could cause the stemming material to fail to seal the hole properly (See Section VI: *Theoretical Considerations*).

Figure V-8 shows tracings of the ANFO/Air to ANFO/Stemming interface taken from the video recordings of each test. It should be noted that the tracings are only two-dimensional sketches of complex three-dimensional interfaces, but a general idea of the processes can be extrapolated from the data. Since the camera angle between the different series of tests of the video recording was not always from the same vantage point, direct comparisons between the series were not possible. Also, some of the camera angles were set up from a front/side view to better see the effect of the interface disturbances. Therefore, some of the original ANFO/Air interfaces appear parabolic due to the tube curvature. A complete set of all the test tracings can be found in Appendix B.

From Figure V-8, it can be seen that as the flow rate of the stemming increased, the degree of disturbance of the interface was greater. The tests also showed that since the final ANFO/Stemming interface was clearly defined, little or no mixing of the ANFO and stemming occurred. One benefit of the tracings in Figure V-8 is that each drawing is inherently to scale, so the degree of disturbance can be quantified. For example, if the diameter of the tube is scaled to the perpendicular measure of each individual tracing, the length and width of the interface disturbances shown can be measured.

From these tests it was found that the original ANFO/Air interface angle did not have a significant effect on the final interface when the stemming was poured at flow rates higher than 1 DV/s. Only at lower flow rates when the ANFO was pushed and then rolled over did it have any effect. Whenever the stemming had enough energy to burrow, the angle and shape of the ANFO/Air interface was insignificant. This helped to decrease the number of following tests since only the relative low and high flow rates of ANFO were necessary for accurate results.



**Figure V-8 -- ANFO/Air vs. ANFO/Stemming Interface Tracings from Video -- S and N Series of Tests.**

### **E. TESTING WITH DIFFERENT TYPES OF STEMMING**

To see if the previous progression of stemming effects were associated with the properties of the sand only, different types of stemming material were tested. The range of materials chosen comprised one material with grain sizes smaller than the ANFO prill, two with sizes greater than the prill, and one with a graded distribution both larger and smaller than the prill. A total of four different materials were used to complete the testing as follows:

For the 1-7/8 in. tube	Medium Sand
For the 3 in. tube	Medium Sand, 1/8 – 1/4 in. Gravel, and Drill Cuttings from a 3.5 in. Hydraulic Drill
For the 4.5 in. tube	1/4 – 3/4 in. Pea Gravel

The sieve analysis of the drill cuttings can be found in Appendix D.

The density of each material used is shown in Table II.

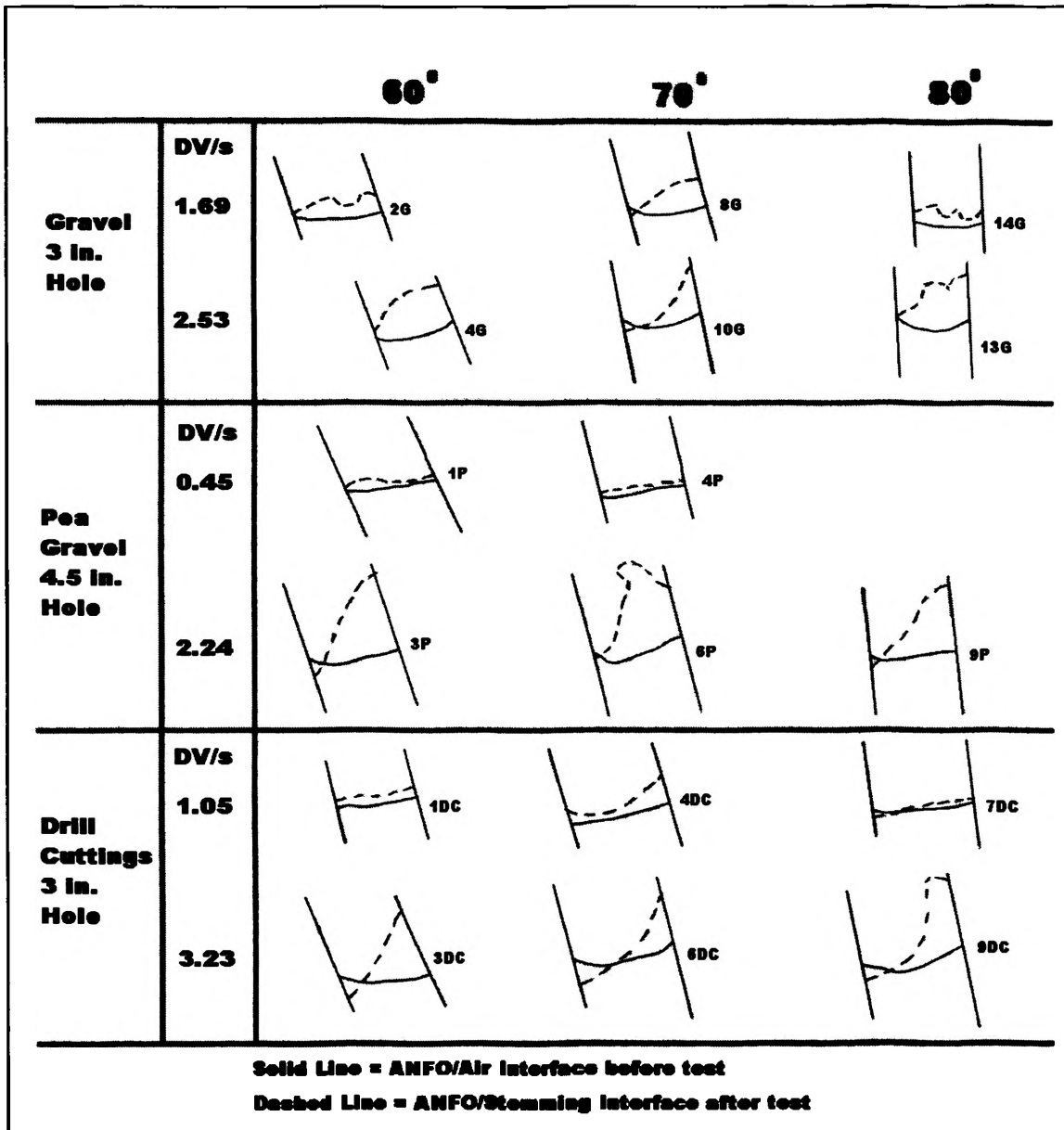
**Table II -- Bulk Densities of Materials Tested**

<b>Material</b>	<b>Density (g/cc)</b>	<b>Test Series Designation</b>
Med. Sand	1.47	S and N
1/8 – 1/4 in. Gravel	1.44	G
1/8 – 1 in. Pea Gravel	1.44	P
Drill Cuttings from 3.5 in. Hyd. Drill	1.65	DC
ANFO	0.88	

(Value for ANFO may be high due to fines created while testing)

The alternate stemming tests included test numbers 1G-17G, 1P-18P, and 1DC-12DC, which were coded for clarification in this analysis. The G series was performed with two flow rates of ANFO and two stemming flow rates, but the P and DC series only used one ANFO flow rate with three different stemming flow rates. The reason for this change in procedure was, as mentioned earlier, because the ANFO flow rates were found to have a minimal effect on the outcome of the tests. The main purpose of these tests was to see if the materials exhibited the same behavior as the sand, and if so, at what flow rates.

Figure V-9 shows selected tracings from each of the series of tests. The tracings in Figure V-9 show a similar progression as shown in Figure V-7 and also occur to a large extent with each new type of stemming material. At lower flow rates, the ANFO/Stemming interface remained relatively flat, while at higher rates, the step function or curved crater surface was evident. Figure V-10 displays images taken from the 8 mm video recordings of each type of stemming before and after a test.



**Figure V-9 – ANFO/Air vs. ANFO/Stemming Interface Tracings from Video – G, P, and DC Series of Tests.**



Figure V-10 – Video Images of Stemming Tests.

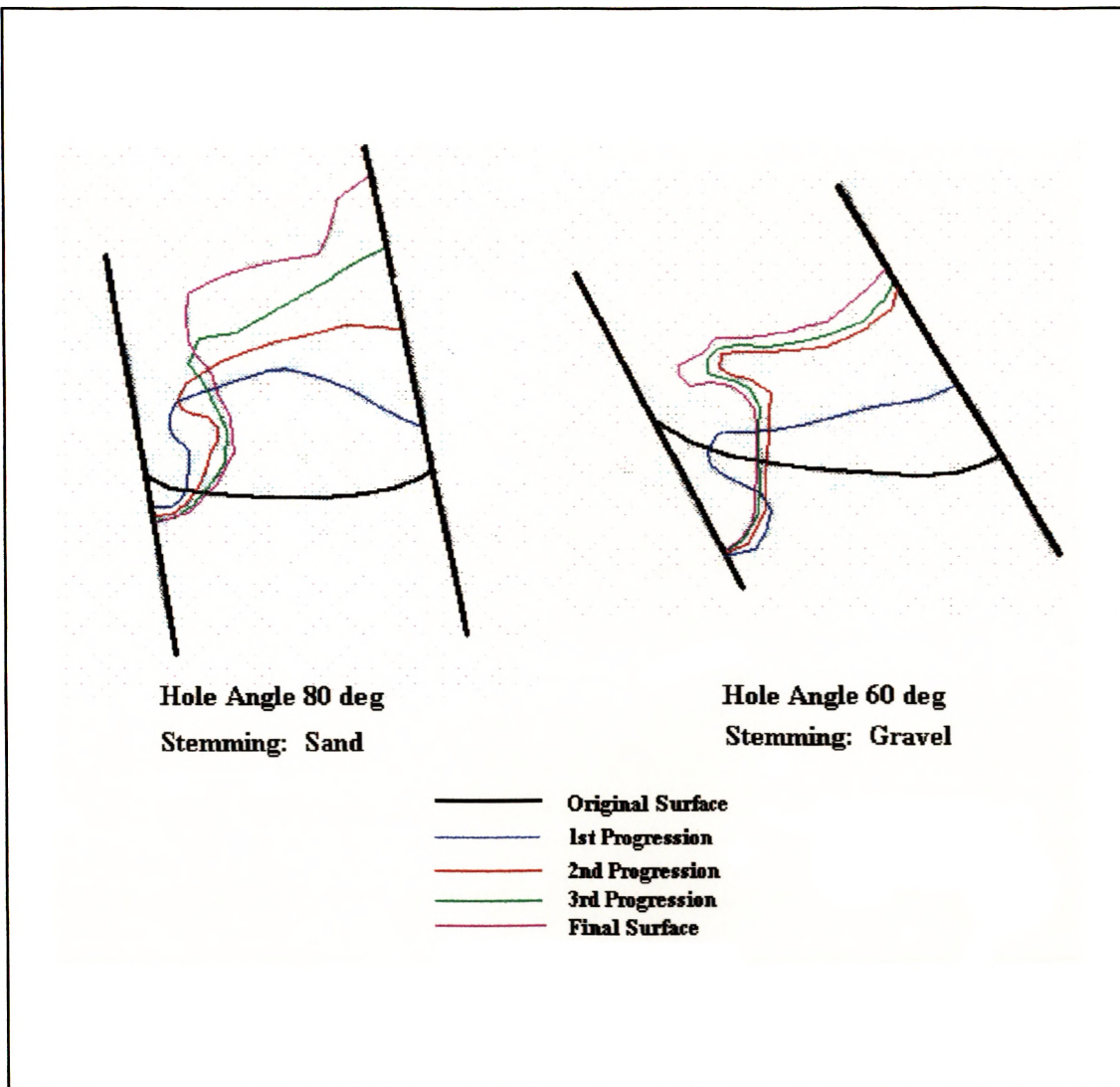


## **F. HIGH-SPEED VIDEO RESULTS**

A total of six tests were performed with the high-speed video camera. Three of the tests were designed to show the mechanisms involved during the high flow rate impacts while the other three were designed to test a theory which will be discussed in subsection H. The high flow rate tests incorporated sand, gravel, and drill cuttings to see if the different grain sizes affected the outcome of the ANFO/Stemming interface during the stemming process.

The results from these tests showed that when any type of stemming material traveled at high flow rates, it would penetrate the ANFO as far as a diameter in length. This literally threw the ANFO grains outward and back up the tube. When the penetration halted, the rest of the stemming material continued to push the ANFO up the tube. At times, grains of ANFO could be found on top of the stemming column. Under the eye of the camera at 500 frames per second, the material interactions seemed almost fluid. Figure V-11 shows tracings of the ANFO/Stemming interface during the stemming process.

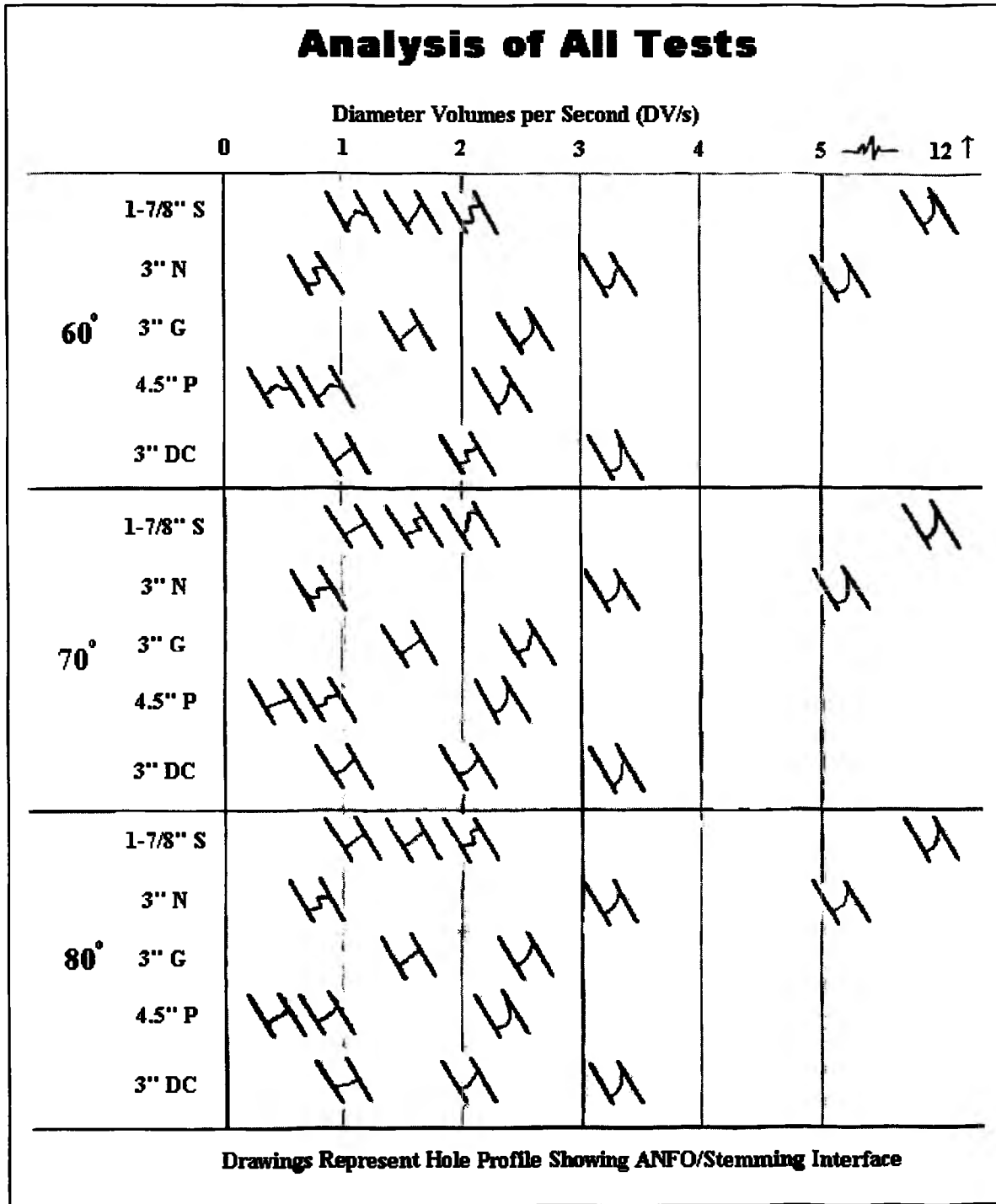
Since the camera angle in Figure V-11 was not parallel to the action, it appears that ANFO is being created since the two dimensional area above the original interface is not equal to the area below. This is just an illusion created by the camera angle. The tracings are pictured at such an angle that the ANFO grains are being thrown right and towards the camera. The progression of this thrust appeared to have a very fluid behavior as noted from the bulbous nature of the interface progressions.



**Figure V-11 -- Tracings of High-Speed Video Tests.**

### **G. ANALYSIS OF ALL TESTS**

With a progression of at least three different types of ANFO/Stemming interfaces, as illustrated in Figure V-7, it was assumed that the different flow rates were responsible for the transitions. However, knowing the precise location of each transition would be beneficial and required for analysis. For this reason, the descriptive graph in Figure V-12 was constructed with the flow rates (DV/s) as the controlling variable.



**Figure V-12 -- Analysis of All Stemming Tests.**

From Figure V-12, it can be seen that regardless of the angle of the tube, the size of the tube, or the type of stemming material, there is a general trend between the shape of the interface and the flow rate as measured in diameter volumes per second. Within a small range of error, the data shows that the step function shape usually occurs between the ranges of 0.8 DV/s and 2 DV/s. Since the step function is the transition between the stemming pushing the ANFO vs. penetrating the ANFO, it is not surprising that below 0.8 DV/s a generally flat or slightly wavy interface is observed, while above 2 DV/s, a curved crater surface is noted.

#### **H. RESULTS DUE TO MODIFICATIONS IN TESTING**

Previous testing involved the addition of the full volume of stemming all at the same time and rate. This allowed for the instances where ANFO grains were lifted up the entire length of the stemming column because the mass was continually entering the system and thus providing the uplift force. When this force was halted for even a half of a second, the outcome of the tests was dramatically altered.

This was discovered after reviewing a few tests that failed because a clump of stemming had hit the ANFO column before the rest of the mass. This occurred because of the effect of increased humidity on the choked 1.5 in. aperture of the 3 in. flow control device during a light drizzle. However, the tests were not failures because the resulting interface was flat and nearly perpendicular to the tube. These were the best results yet. It was already concluded that a smaller mass of lower flow rate material would ultimately be in the final recommendations, but confirmational testing was necessary to support this. To further explore this phenomenon, the last three tests of each series were altered to

recreate this effect to see if it was repeatable. High-speed video of the process was also recorded.

From the modified tests, it was found that it took a minimum amount of stemming material in the initial clump to give the desired results. This volume was estimated to be around 0.5 DV (diameter volumes). Above and below this volume, the tests gave similar results to previous tests, showing a complex interface depending upon the flow rate.

The high-speed video analysis was helpful in determining the reason for this modification being successful. As the initial clump hits the ANFO, there was not enough mass to penetrate the prill, so it only pushed the interface into a flat surface that was roughly perpendicular to the tube. A certain required volume of the clump was then necessary to act as a shield for the ANFO/Stemming interface. When the rest of the stemming was poured onto this layer, it burrowed into the clump only, leaving the interface untouched. The stemming could not burrow as deeply into the clump as it did into the ANFO because the clump was the same density as the incoming mass, which was significantly greater than the ANFO. The required volume was again determined to be about 0.5 to 0.75 DV (diameter volumes). Figure V-13 shows the results of these tests.

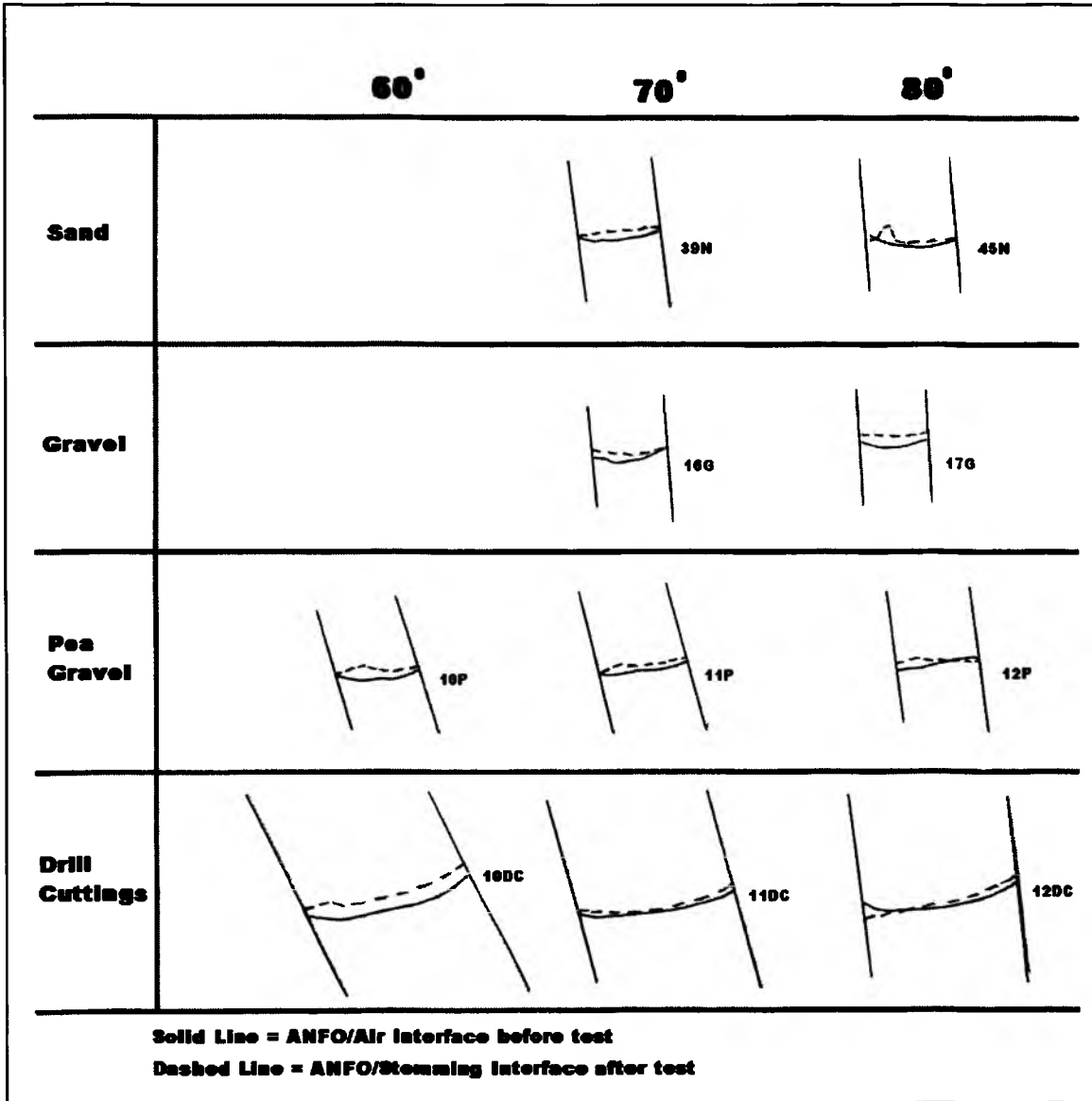


Figure V-13 -- Tracings of Modified Tests.

## ***VI. THEORETICAL CONSIDERATIONS***

### ***A. PENETRATION POTENTIAL***

The main difference between loading an angled hole compared to a vertical hole is that the material poured into the hole will naturally tend to slide along the footwall of the hole instead of dispersing across the whole cross-section in a complete freefall. As the angle increases towards the horizontal, the frictional force from the sliding particles will increase as more weight is applied to the footwall surface, and the gravitational component in line with the hole will decrease. Equilibrium will be reached when the particles no longer flow down the length of the hole.

Stemming, when loaded into a blast hole, should behave in a manner similar to ANFO. This, however, may be the cause of the burrowing behavior that was witnessed in the tests. When the stemming material is introduced into a vertical hole, the mass is spread across the entire area of the hole. For an angled hole, the mass concentrates near the footwall into a smaller area, and as the area decreases, the pressure exerted by the stemming mass increases. This pressure increase raises the potential for penetration, however, the penetration is dependent upon the mass relationship of the bulk densities, and the average velocity of the penetrating material. Of course, the velocity of the material will decrease with the hole angle as it approaches horizontal as a result of increasing frictional drag. This means a range of angles can be calculated where the concentration of area is maximized, and the velocity is still high enough to cause the most penetration.

A higher flow rate only increases the velocity up to a point where the gravitational limit is met, then increasing the flow rate only increases the area. This larger area generally limits the penetration, and some of the results of the tests showed that medium-high flow rates penetrated the deepest into the ANFO column, while the fastest flow rates penetrated the same, but left less volume in the ANFO stringer thrown up the hanging side of the tube (e.g. Tests 20N and 22N).

#### **B. POTENTIAL COMPLICATIONS ARISING FROM A NON-IDEAL INTERFACE**

When the final ANFO/Stemming interface is not flat and perpendicular to the blast hole, there are two problems that theoretically may occur. From the complex interfaces that were discovered in this research, it was clear that in a non-ideal interface, there was a region where the ANFO did not completely span the entire hole in a perpendicular direction. Whether in a thin streamer up the side of the hole, or in a shortened clump, the explosive was not arranged as designed. The potential problems resulting from this segregated ANFO are:

1. This smaller volume will become insensitive when its thickness falls below the critical diameter of ANFO, significantly reducing the shock energy component of the segregated ANFO, and thereby reducing the potential energy in the blast hole which lowers efficiency.
2. The smaller volume, since it does not span the entire hole, may still detonate, but may also induce a horizontal component of compression within the blast hole instead of into the surrounding rock. This can cause the stemming material to be less effective, and thus decrease the efficiency of the blast.

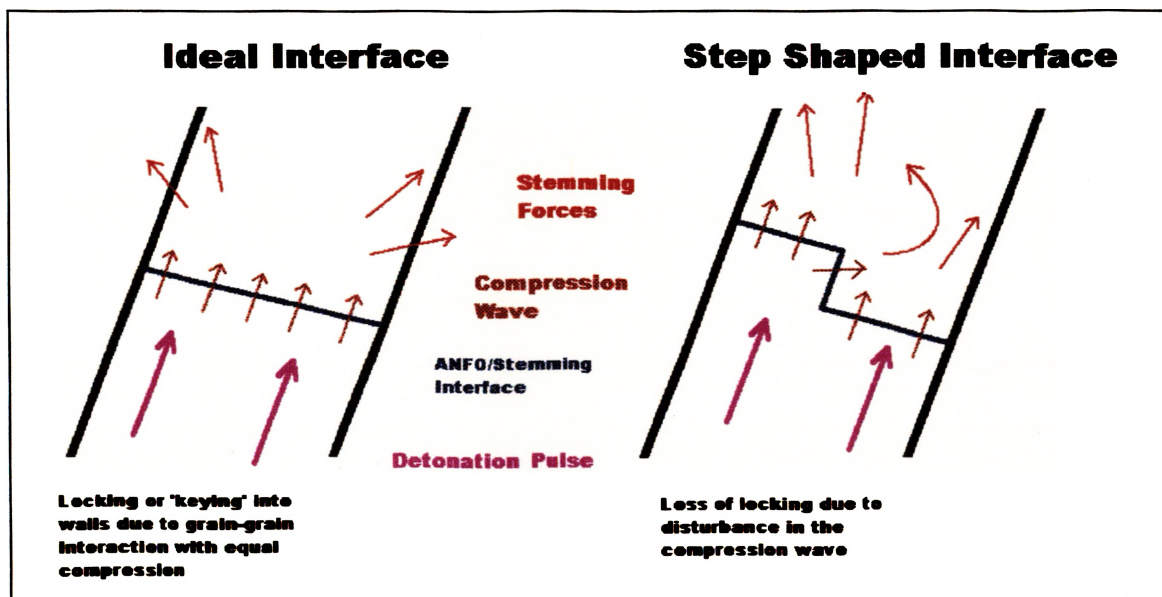


While the first problem is easily visualized, the second problem will need further explanation. This potential problem would probably occur in the middle interface of the defined progression (See Figure V-7) which takes the form of a step function. The segregated mass of ANFO has a diameter close to half the diameter of the hole, so unless the hole diameter is small scale, the mass will be greater than the critical diameter of ANFO. For this reason, the step function interface will be used to illustrate this theory.

First of all, an ANFO column is typically detonated from the bottom of the blasthole, so the detonation pulse will come from bottom of the hole, and progress parallel to the hole. After the detonation pulse, the explosive gases exert pressure in all directions away from the explosive column. Near the interface of the ANFO and the stemming, the energetic gases tend to exert pressures both into the surrounding rock and upwards into the stemming column. If the interface is perpendicular to the blasthole, then the uppermost pressures will exert a compression wave parallel to the blasthole into the stemming column. This equal pressure along the whole bottom area of the stemming column is distributed into the stemming material. Since the stemming material is angular, the forces are redirected within the mass and transferred into interactions between the surrounding rock and the individual particles of stemming. These interactions are responsible for the stemming locking or keying into the surrounding rock, thereby making it difficult for the explosive gases to escape through the top of the blasthole. With the gases held in the hole, the only avenue for escape is through the surrounding rock that is designed to be blasted.

However, if the interface is shaped like the step function, the compression wave will not exert equal pressure on the bottom area of the stemming column. A horizontal

component is created inside the hole due to the fact that the detonation pulse is faster than the velocity of the explosive gases after detonation. As the detonation pulse hits the ANFO contained in the upper part of the step, the same forces are exerted, however a component of these forces go into the stemming, both perpendicular to the hole as well as parallel to the hole. As the pressure from the lower interface of the step meets with this horizontal component, a resultant pressure is created neither parallel nor perpendicular to the hole. Figure VI-1 shows a pictorial representation of this theoretical phenomenon.



**Figure VI-1 -- Pictorial Representation of Theoretical Stemming Problem.**

As seen in Figure VI-1, the impact of the unequal pressure on the stemming column may cause the stemming to lose a part of the locking potential that seals the explosive gases within the hole. An analogy would be trying to force an angular block through a hole that is not quite big enough to allow free passage. Pushing with equal

force on the block will prove ineffective if the block is obstructed by its angular nature. However, pushing the block and rotating it until a smaller diameter is found in the angular mass may succeed in pushing the block through the hole. This may also be true of the stemming material in the blasthole. If the force on the stemming material is exerted equally, then the angularity of the material will lock into the surrounding rock and provide resistance to the explosive gases. However, if the force on the stemming material is not equal, then a rotational component of the exerted force may disturb the effectiveness of the stemming as it tries to lock into the surrounding rock. Without the locking ability, the stemming may become fluidized by the explosive gases, increasing the likelihood of stemming ejection from the hole, thereby allowing the explosive gases to be released prematurely. If the gases are released out of the top of the blast hole instead of into the rock designed to be blasted, then the blast will be less efficient.

## ***VII. CONCLUSIONS***

From this research, several conclusions have been drawn about the loading processes of ANFO and stemming in inclined holes. The results of the tests has helped to further explain the nature of the ANFO loading processes and the interactions that occur between the ANFO and stemming material during the stemming of an inclined hole.

The conclusions derived from this research, in chronological order, are as follows:

- The flow rate of the ANFO during the loading process controls the complexity and angle of the final surface.
- A higher flow rate of ANFO will result in a final angle closer to perpendicular to the hole than that of a lower flow rate.
- The flow rate of ANFO controls the mechanism of flow during loading. With a higher flow rate, there is more potential for burrowing or undercutting.
- Separation of grain sizes (coarse on top) occurs when undercutting processes exist during loading.
- As stemming is introduced in the system, a defined progression of shapes of the interface occurs that depend upon the flow rate of the stemming.
- Regardless of the stemming material or its size, the same defined progression exists, but slight variations in intensity of the effects can be observed.
- The variations in intensity are believed to be related to the relative bulk density of the stemming material, i.e. a higher density material will penetrate deeper than lower density materials at the same flow rates.
- The three types of interfaces noted in the progression of shapes can be delineated with respect to the flow rate of the stemming as measured in diameter volumes per second. Other factors, such as hole angle, size of hole, and original ANFO/Air interface, have minimal effect.
- A combination of the slow pouring of a small volume (0.5 to 0.75 DV) of stemming then fast loading of the rest of the stemming volume results in the most ideal ANFO/Stemming interface.

From this research, it was found that stemming processes for angled holes are more complex than originally believed. The tests show that the factors which control the angle and shape of the final interface of the ANFO and stemming are as follows, in order of increasing significance:

- The flow rate of the ANFO loading, especially the last portion;
- The angle of the blast hole with respect to vertical;
- The size distribution and density of the stemming used;
- The flow rate of the initially introduced stemming material;
- The volume of the initially introduced stemming material loaded.

The last two factors, flow rate and volume of initial stemming, have the most direct influence on the shape and angle of the final interface. Manipulating these factors alone can greatly change the outcome of the interface. This correlates favorably with continuing research with different types of stemming (See Section III: *Previous Work*). The type and size of stemming has little effect, however, the way the stemming is loaded is critical in the formation of the final interface between the ANFO and the stemming.

### ***VIII. RECOMMENDATIONS***

Based upon the results from this research, the list below shows the recommended loading steps for an optimum ANFO/Stemming interface for an inclined hole charged with ANFO. The optimum interface consists of a flat surface that is as close to perpendicular as possible to the length of the blast hole. The sequence of steps given below are manipulations of the loading and stemming processes necessary to achieve this:

- Load ANFO into hole as fast as possible, especially concentrating on loading the final portion quickly.
- Slowly load approximately 0.5 to 0.75 Diameter Volumes of stemming at a flow rate of under 1 Diameter Volume per second.
- Pause between the initial stemming and the rest of the stemming for at least one half of a second to stabilize the system.
- Continue loading the rest of the stemming at any desired rate.

## ***IX. FURTHER STUDIES***

The scope of this research effort was changed during the course of the tests in order to focus on the effects of loading inclined holes only at angles not more than thirty degrees from vertical. This leaves ample room for further studies on loading processes of ANFO and stemming. A list of topics that the author deems worthy of further research and testing is as follows:

- Attempt to quantify the loss of efficiency in a blasthole caused by complex interfaces described in this thesis, such as the step shaped interface discussed in Section VI: *Theoretical Considerations*.
- Study the practicality of stemming horizontal holes, plus a study of the final interfaces between the ANFO and the stemming after the mechanical loading of horizontal holes.
- Conduct an efficiency study to determine the effects, if any, of gradation of ANFO prill during the loading of inclined holes.

*APPENDIX A*

**RESULTS OF EACH TEST SERIES**



**Table A-I -- Descriptions of Test Series**

<b>Test Series</b>	<b>Testing Parameters</b>
Numbered Series	1-7/8 in. Tube ANFO loading only
S- Series	1-7/8 in. Tube Stemming: Sand
N- Series	3 in. Tube Stemming: Sand
G- Series	3 in. Tube Stemming: 1/8 to 1/4 in. Gravel
P- Series	4.5 in. Tube Stemming: 1/4 to 3/4 in. Pea Gravel
DC- Series	3 in. Tube Stemming: Drill Cuttings



Table A-III -- Results of Tests 27-49

Test	Series	Tube Angle (from Vert)	ANFO Flow Rate DV/s	ANFO/Air Deviation Angle (from Parallel)	Test	Series	Tube Angle (from Vert)	ANFO Flow Rate DV/s	ANFO/Air Deviation An (from Para
27		40	0.7	27	43		30	12.6	53
28		45	0.7	20	44		40	12.6	48
29		50	0.7	14	45		50	12.6	23
30		55	0.7	4	46		55	12.6	15
31		60	0.7	1	47		55	12.6	14
32		30	1	45	48		60	12.6	6
33		40	1	29	49		65	12.6	N/A
34		45	1	28					
35		50	1	24					
36		55	1	9					
37		30	1.45	53					
38		40	1.45	42					
39		45	1.45	34					
40		50	1.45	29					
41		55	1.45	19					
42		60	1.45	5					

Table A-IV -- Results of Tests 1S-13S








Test	Series	Tube Angle (from Vert)	ANFO Flow Rate DV/s	ANFO/Air Deviation Angle (from Parallel)	Stemming Flow Rate DV/s	ANFO/Stemming Deviation Angle (from Parallel)	Drawings -- Notes
1	S	40	0.7	34	0.35		not much change, but forgot to measure
2	S	40	0.7	34	0.64		41° some undermining
3	S	40	0.7	34	1.15		the 34° held at the top, undermining large  effective change past perp.
4	S	40	0.7				camera died, screwed up filming also, decided to do 2 and 3 over again
2	Sa	40	0.7	33	0.64		38° more undermined this time
3	Sa	40	0.7	33.5	1.15		same notes as 3S
4	Sa	40	0.7	30	1.58		half of tube undermined 2 in. 
5	S	40	0.7	34	2.05		couldn't undermine as much due to large mass of flow  strange shape
6	S	50	0.7	9	0.35		9° no real change
7	S	50	0.7	9	1.15		17° some undermining
8	S	50	0.7	11	2.05		29° kicked it good, packed it 
9	S	30	0.7	43	1.15		forgot
10	S	30	0.7	43	1.58		50° and 163° undercut 
11	S	30	0.7	42.5	2.05		43° on top, 1 x 1 in. undercut 
12	S	30	0.7	43	12.85		major underswirl, flattened top 
13	S	20	0.7	60	1.15		125° kicked angle back

Table A-V -- Results of Tests 14S-28S








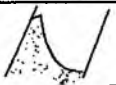
Test	Series	Tube Angle (from Vert)	ANFO Flow Rate DV/s	ANFO/Air Deviation Angle (from Parallel)	Stemming Flow Rate DV/s	ANFO/Stemming Deviation Angle (from Parallel) + Drawings - Notes
14	S	20	0.7	63	1.58	116°
15	S	20	0.7	55	2.05	130° angle perp. to view 
16	S	20	0.7	56	12.85	139° bad undercut
17	S	20	12.6		1.15	96°
18	S	20	12.6		1.58	 Area 1.5 x 1.5 in.
19	S	20	12.6		2.05	 35° and 130°
20	S	20	12.6		12.85	 curved
21	S	10	12.6		1.15	104°
22	S	10	12.6		1.58	99°
23	S	10	12.6		2.05	 3/4 x 3/4 in. Area
24	S	10	12.6		12.85	109°
25	S	30	12.6		1.15	 37° and 157°
26	S	30	12.6		1.58	119° with some remnant upsurge of ANFO
27	S	30	12.6		2.05	58°  0.5 x 1.5 in. Area
28	S	30	12.6		12.85	 roughly 130°, but curved

Table A-VI -- Results of Tests 1N-16N




Test	Series	Tube Angle (from Vert)	ANFO Flow Rate DV/s	ANFO/Air Deviation Angle (from Parallel)	Stemming Flow Rate DV/s	ANFO/Stemming Deviation Angle (from Parallel)	Drawings - Notes
1	N	10	0.17	57	3.14	 Bowed 0.5 in. in middle	
2	N	10	0.25	61	3.14	117° little curve	
3	N	10	0.35	67	3.14	84°	
4	N	10	3.08	80	3.14	130° curved surface	
5	N	20	0.17	48	3.14	kicked all the way over, some ANFO on top of stemming 	
6	N	20	0.25	55	3.14	same as last, but thicker on the right	
7	N	20	0.35	55	3.14	140° on backside, huge scoop out	
8	N	20	3.08	76	3.14	The kick was skewed a little, but basically the same as last	
9	N	30	0.17	39	3.14	Huge kick on opposite side of camera view	
10	N	30	0.25	40	3.14	same result as last	
11	N	30	0.35	47	3.14	same, it seems that the stemming is taking a serpentine shaped path down the tube, so it is not hitting directly square in relation to the camera angle.	
12	N	30	3.08	61	3.14	same	
13	N	30	3.08	67	0.2	68° small notch burrowed, but not much	
14	N	30	3.08	67	0.4	70° on right side  average across tube is 84°	
15	N	30	3.08		0.6	not too much plateaus, looked good	
16	N	20	3.08	76	0.2	little bit wavy, but near perpendicular	

Table A-VII -- Results of Tests 17N-32N













Test	Series	Tube Angle (from Vert)	ANFO Flow Rate DV/s	ANFO/Air Deviation Angle (from Parallel)	Stemming Flow Rate DV/s	ANFO/Stemming Deviation Angle (from Parallel) + Drawings - Notes
17	N	20	3.08	76	0.4	99°
18	N	20	3.08	76	0.6	undercut in front (snaked), sizable cut
19	N	30	0.8	53	0.8	
20	N	30	0.8	52	3.13	
21	N	30	0.8	52	3.18	
22	N	30	0.8	52	5.27	
23	N	30	3.18	68	0.8	
24	N	30	3.18	68	3.13	 some extra kick on backside, but not much
25	N	30	3.18	69	3.18	about same as last, but more kick up
26	N	30	3.18	68	5.27	still more volume of kickup, some ANFO at the top of the stemming
27	N	3	5.27	70	0.8	 looked good, not much disturbance in back
28	N	30	5.27	68	3.13	 side  ← from top view though lots of kick up
29	N	30	5.27	70	3.18	 stringer in back, 0.5 in. width
30	N	30	5.27	69	5.27	 small volume in back stringer
31	N	20	0.8	64	0.8	 remnant of ANFO got scooped up, interesting process
32	N	20	0.8	64	3.13	scooped a piece to the backside + a small peak

Table A-VIII -- Results of Tests 33N-48N



Test	Series	Tube Angle (from Vert)	ANFO Flow Rate DV/s	ANFO/Air Deviation Angle (from Parallel)	Stemming Flow Rate DV/s	ANFO/Stemming Deviation Angle (from Parallel)	Drawings -- Notes
33	N	20	0.8	64	3.18	threw ANFO on top	** changing camera angle to see both the side and top of the tube **
34	N	20	0.8	64	5.27	large throw in back	
35	N	20	3.18	73	0.8	mess up in test, a little bit fell before the main volume, however, this was the best interface angle yet	
36	N	20	3.18	73	3.13	strange peak in front	
37	N	20	3.18	80	3.18	large kick up	
38	N	20	3.18	77	5.27	↑ again	1.5 in. nozzle causing trouble
39	N	20	5.27	87	0.8	accident again, but the angle was nearly perpendicular the second wave scooped up sand this time instead of ANFO, leaving the interface untouched	
40	N	20	5.27	85	3.13	2 in. high scoop out	
41	N	20	5.27	84	3.18	a little extra gouged out in back, plus some kick up in the front	
42	N	20	5.27	84	5.27		
43	N	10	0.8	66	0.8		the old step -- have we seen this before?
44	N	10	0.8	71	3.13	threw up a little on top of stemming	
45	N	10	0.8	70	3.18	I believe a clump hit the ANFO again, the interface was flat and perpendicular	
46	N	10	0.8	70	5.27	very flat surface, looked good	
47	N	10	3.18	79	0.8	clump effect once again	Tests affected by humidity, it was lightly raining, sand was getting wetter
48	N	10	3.18	77	3.13	little bit of scoop, mostly flat	test 49 and 50 were worthless, then stopped due to rain



Table A-IX -- Results of Tests 1G-16G



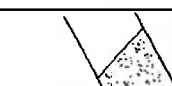


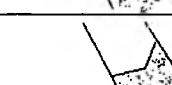

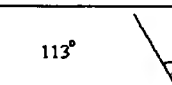







Test	Series	Tube Angle (from Vert)	ANFO Flow Rate DV/s	ANFO/Air Deviation Angle (from Parallel)	Stemming Flow Rate DV/s	ANFO/Stemming Deviation Angle (from Parallel) + Drawings - Notes
1	G	30	3.13	72	2.53	 shootup 2.5 in.
2	G	30	3.13	72	1.69	 108° flat interface
3	G	30	3.13	72	2.56	112° flat
4	G	30	5.27	60	2.53	 120° flat
5	G	30	5.27	60	1.69	 105° flat
6	G	30	5.27	60	2.56	 100° bumpy, but mostly flat
7	G	20	3.13	81	2.53	 about 2 in. throw up in back, thin
8	G	20	3.13	82	1.69	114° flat
9	G	20	3.13	80	2.56	kind of spiral tilt avg angle 120°
10	G	20	5.27	80	2.53	95° with 3 in. kickup in backside
11	G	20	5.27	80	1.69	same
12	G	20	5.27	43	2.56	same
13	G	10	3.13	84	2.53	 curved with 2 in. kickup
14	G	10	3.13	84	1.69	94° flat, excellent interface
15	G	10	3.13	94	2.56	113° 
16	G	20	5.27	83	Slow/Fast	90° flat and perp. -- looks like the modifications work

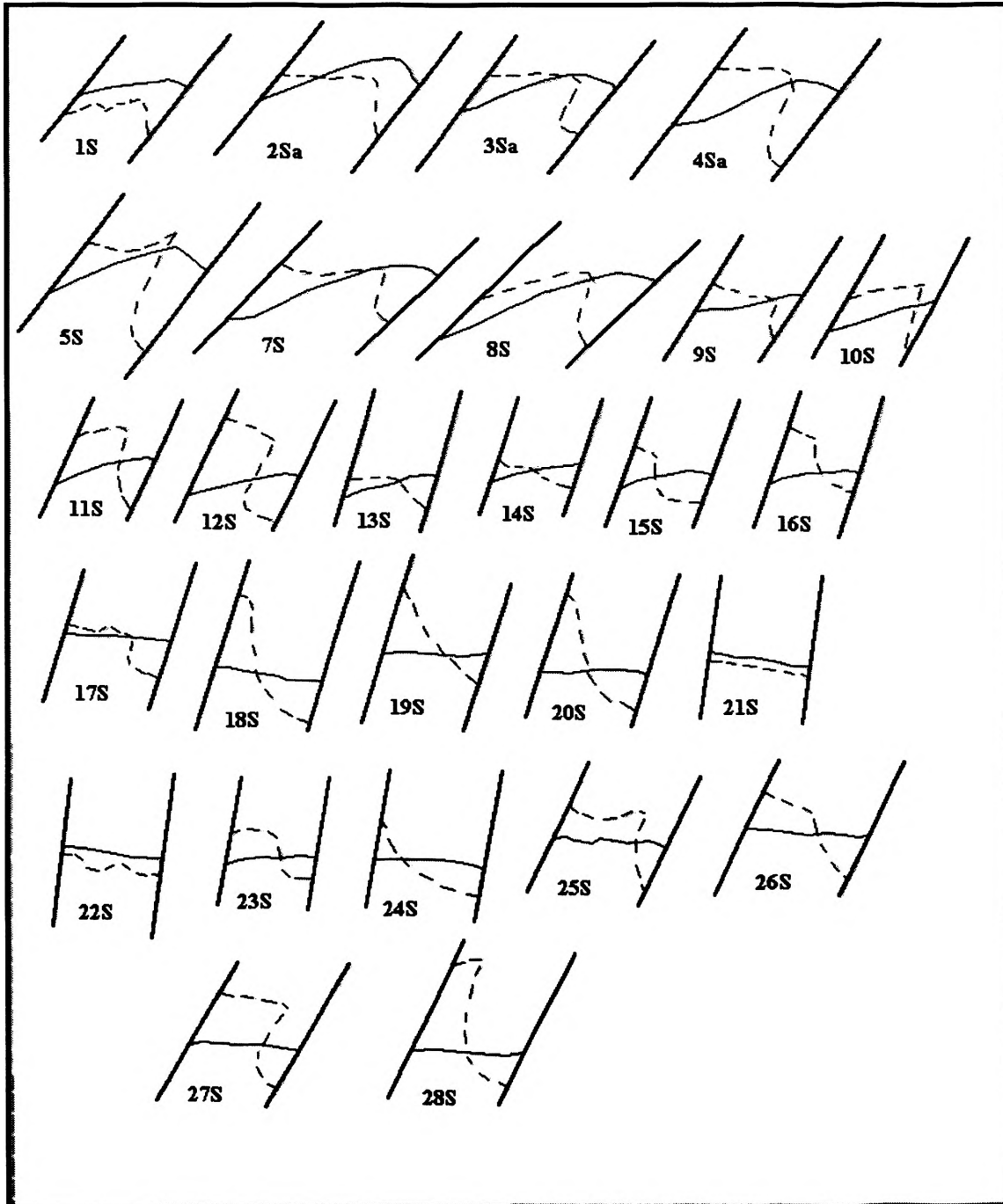
Table A-X -- Results of Tests 17G and 1P-12P

Test	Series	Tube Angle (from Vert)	ANFO Flow Rate DV/s	ANFO/Air Deviation Angle (from Parallel)	Stemming Flow Rate DV/s	ANFO/Stemming Deviation Angle (from Parallel) + Drawings -- Notes
17	G	10	3.13	89	Slow/Fast	95° flat -- excellent
1	P	30	> 6.0	72	0.45	 mainly 89° with 1.75 in. hump on both sides (sym)
2	P	30	> 6.0	65	0.66	 107° with 1 in. hump -- some penetration
3	P	30	> 6.0	72	2.24	 large burrow, threw ANFO on top of stemming
4	P	20	> 6.0	87	0.45	96° straight contact
5	P	20	> 6.0	87	0.66	 90° small step function (1 in.)
6	P	20	> 6.0	85	2.24	burrowed deep, threw ANFO up again onto stemming
7	P	10	> 6.0	94 ?	0.45	102° straight
8	P	10	> 6.0	87	0.66	105° 
9	P	10	> 6.0	91	2.24	highly ballistic same as the other angles 
10	P	30	> 6.0	69	Slow/Fast	not enough rock in initial dump, but still was better than the normal pour
11	P	20	> 6.0	81	Slow/Fast	 96° worked good, only small 0.5 in. hump
12	P	10	> 6.0	85	Slow/Fast	98° straight -- excellent

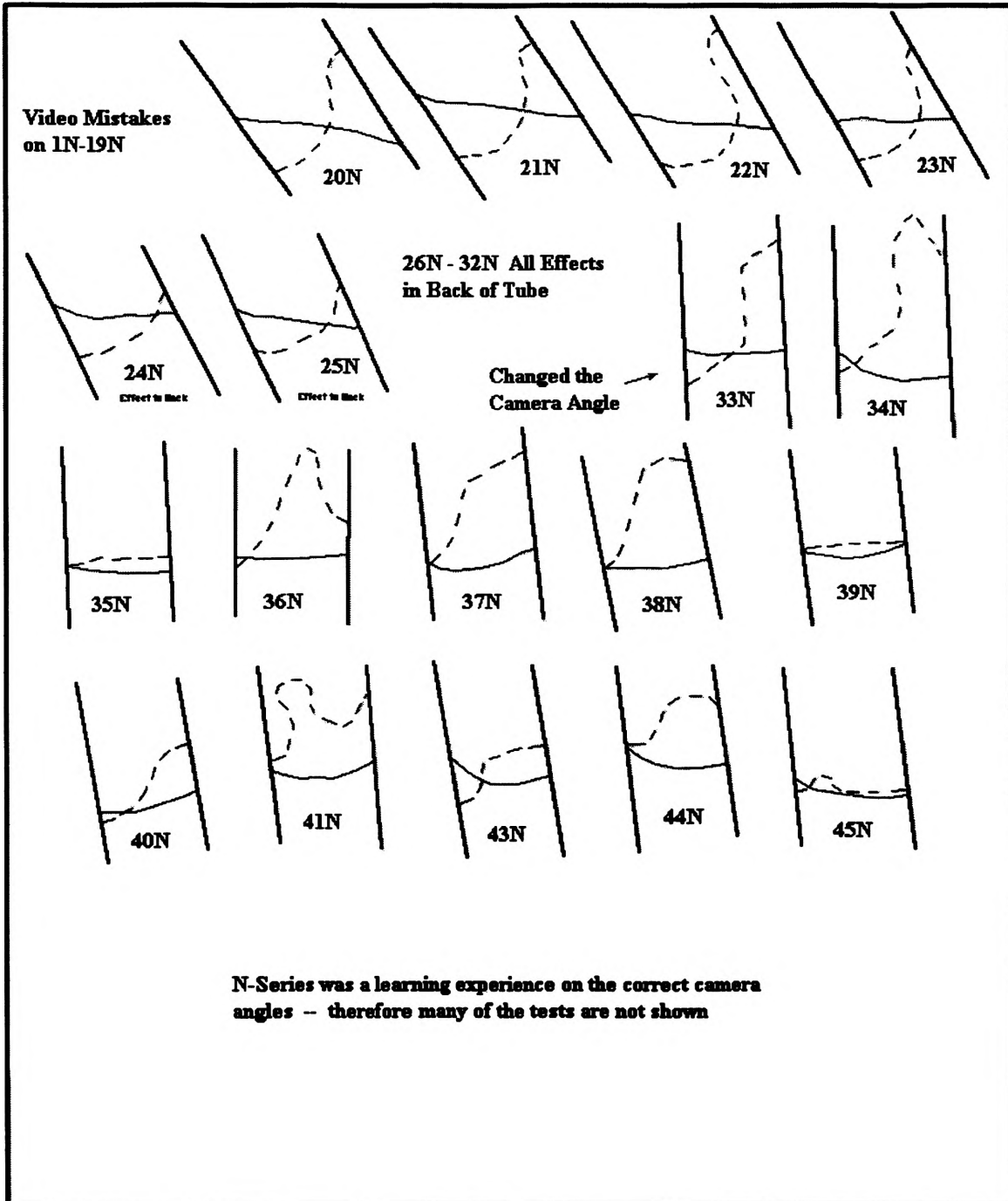


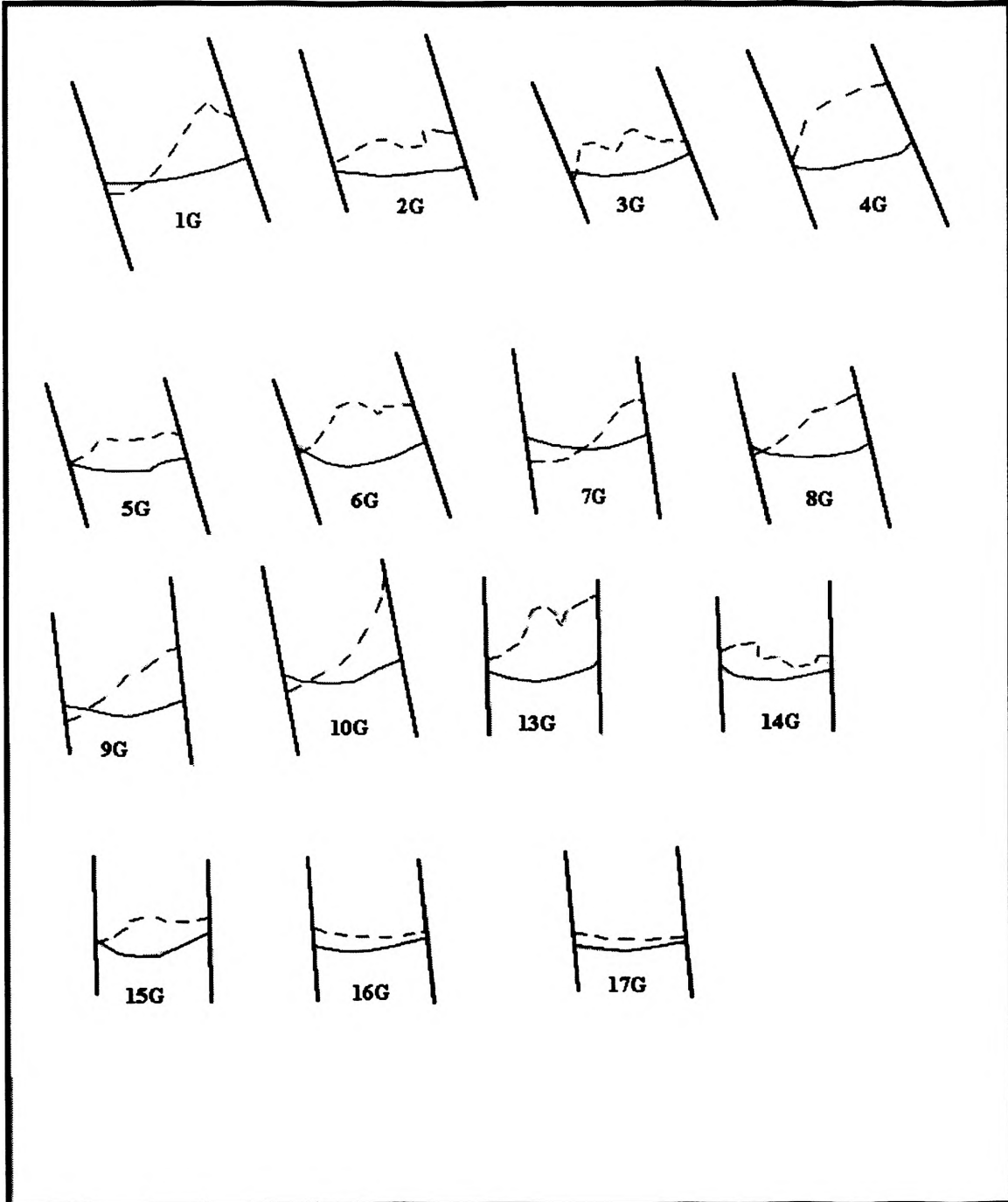
***APPENDIX B***

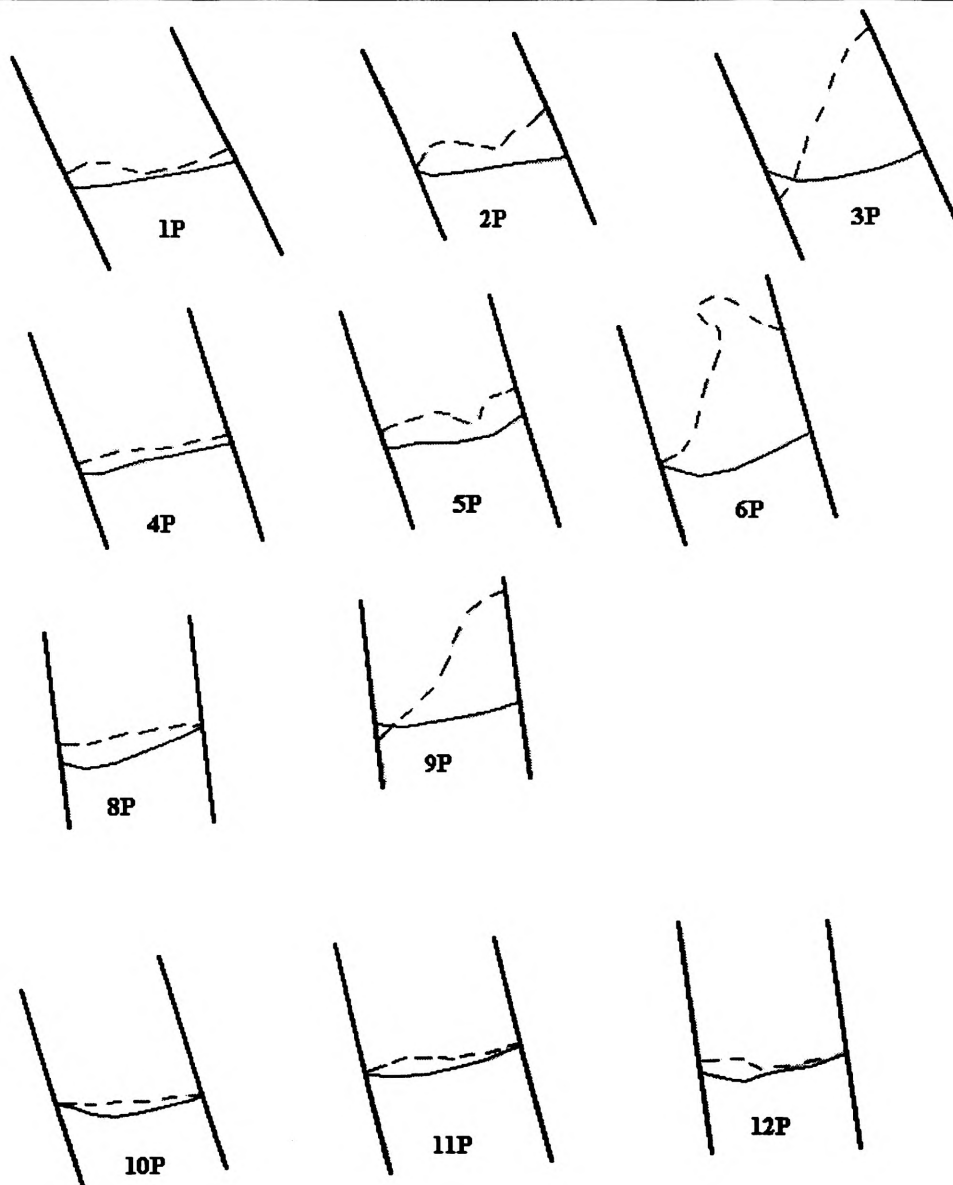
**VIDEO TRACINGS OF ALL TESTS**

**Table B-I -- Video Tracings of S- Series Tests**

**Table B-II -- Video Tracings of N- Series Tests**

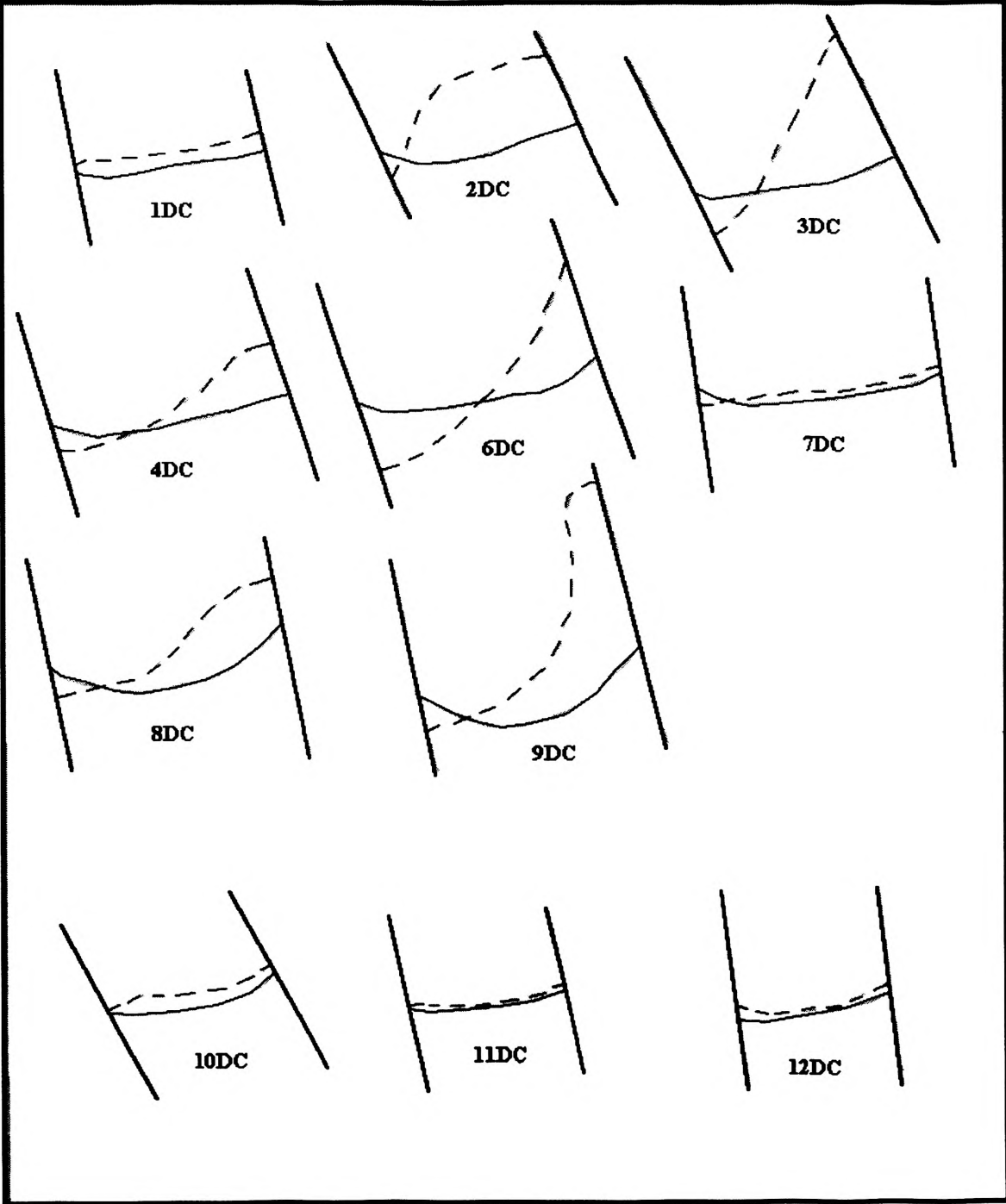


**Table B-III -- Video Tracings of G- Series Tests**

**Table B-IV -- Video Tracings of P- Series Tests**



**Table B-V -- Video Tracings of DC- Series Tests**



***APPENDIX C***

**FLOW RATE EQUATIONS AND SPREADSHEETS**

Table C-I -- Calculated Flow Rates of Each Material

Flow Rates for each material									
Sand									
1/2 in					5/8 in				
ml	500	1000	1500	2000	ml	500	1000	1500	2000
time	16.61	33.47	50.03	66.71	time	9.03	17.79	27.14	36.87
Calculations					Calculations				
30.10235	29.65599	30.08424			55.37099	57.07763	52.9881		
29.8775	30.19324	29.94012	avg. =	29.97	56.21135	53.47594	54.26918	avg. =	54.69
29.98201	29.9222			mL/s	55.26898	55.21811			mL/s
29.98051	29.97802				54.5405	52.4659			
3/4 in					7/8 in				
ml	500	1000	1500	2000	ml	500	1000	1500	2000
time	4.9	10.14	15.2	20.6	time	3.59	7.39	13.11	15.2
Calculations					Calculations				
102.0408	95.41985	95.60229			139.2758	131.5789	128.041		
98.61933	98.81423	95.5414	avg. =	97.15	135.318	87.41259	129.199	avg. =	134.11
98.68421	97.08738			mL/s	114.4165	105.042			mL/s
97.08738	92.59259				131.5789	239.2344			
1 in					1.5 in				
ml	500	1000	1500	2000	ml	500	1000	1500	2000
time	2.77	5.69	8.52	11.54	time	1.55	3.33	5.21	7.2
Calculations					Calculations				
180.5054	171.2329	170.9402			322.5906	280.8989	258.3979		
175.7469	176.6784	171.0376	avg. =	173.50	300.3003	265.9574	265.4667	avg. =	278.38
176.0563	173.913			mL/s	287.9079	273.224			mL/s
173.3102	165.5629				277.7778	251.2563			
2 in					2.5 in				
ml	1000	2000	3000		ml	1000	2000	3000	
time	0.82	1.85			time	0.79	1.83		
Calculations					Calculations				
1219.512	970.8738				1285.823	981.5385			
1081.081			avg. =	1090.49	1092.886			avg. =	1106.75
				mL/s					mL/s
2.6 in					3 in				
ml	1000	2000	3000		ml	1000	2000	3000	
time	0.49	1.1			time	0.39	0.81		
Calculations					Calculations				
2040.816	1639.344				2684.103	2390.952			
1818.182			avg. =	1832.78	2469.136			avg. =	2471.40
				mL/s					mL/s

Table C-I -- Calculated Flow Rates of Each Material (continued)

<b>Gravel</b>									
<b>2 in</b>					<b>2.3 in</b>				
ml	1000	2000	3000		ml	1000	2000	3000	
time	1.11	2.28			time	1.64	3.41		
Calculations					Calculations				
900.9009	854.7009				609.7561	564.9718			
877.193			avg. =	877.60	586.5103			avg. =	587.08
				mL/s					mL/s
<b>2.6 in</b>									
ml	1000	2000	3000						
time	1.11	2.23	3.37						
Calculations									
900.9009	892.8571								
896.861	877.193		avg. =	890.50					
890.2077	884.9558			mL/s					
<b>Pea gravel</b>									
<b>2.3 in</b>					<b>2.6 in</b>				
ml	1000	2000	3000		ml	1000	2000	3000	
time	1.52	3.55	5.75		time	0.98	1.99		
Calculations					Calculations				
657.8947	492.6108				1020.408	990.099			
563.3803	454.5455		avg. =	527.16	1005.025			avg. =	1005.18
521.7391	472.8132			mL/s					mL/s
<b>3 in</b>									
ml	1000	2000	3000						
time	0.38								
Calculations									
2631.579			avg. =	2631.58					
				mL/s					
<b>Drill cuttings</b>									
<b>2 in</b>					<b>2.3 in</b>				
ml	1000	2000	3000		ml	1000	2000	3000	
time	1.48	3.72	5.55		time	2.8	5.58	8.25	
Calculations					Calculations				
675.6757	448.4286				357.1429	359.7122			
537.6344	548.4481		avg. =	539.69	358.4229	374.5318		avg. =	363.40
540.5405	491.4005			mL/s	363.6364	368.9725			mL/s
<b>2.6 in</b>					<b>3 in</b>				
ml	1000	2000	3000		ml	1000	2000	3000	
time	1.38	2.85			time		1.72	2.65	
Calculations					Calculations				
724.6377	680.2721				1162.791	1075.269			
701.7544			avg. =	702.22	1132.075			avg. =	1123.38
				mL/s					mL/s

**Table C-II -- Calculations for Diameter Volumes per Second**

<b>Diameter Volumes per Second</b>							
				Diameter	1-7/8"	3"	4.5"
				volumes	84.84	347.50	1172.81 mL/DV
For 1-7/8's in tube							
			Nozzle Diameters				
Sand	1/2 in	5/8 in	3/4 in	7/8 in	1 in	2 in	
	0.353275	0.644592	1.1451	1.580758	2.045034	12.85365	
For 3 in tube							
			Nozzle Diameters				
Sand	1.5 in	2 in	2.3 in	2.6 in			
	0.80109	3.138098	3.184899	5.27419			
For 3 in tube							
			Nozzle Diameters				
Gravel	2 in	2.3 in	2.6 in				
	2.525463	1.689437	2.562578				
For 3 in tube							
			Nozzle Diameters				
Drill cuttings	2.3 in	2.6 in	3 in				
	1.045764	2.020781	3.232743				
For 4.5 in tube							
			Nozzle Diameters				
Pea Gravel	2.3 in	2.6 in	3 in				
	0.449487	0.857066	2.243819				

***APPENDIX D***

**BULK DENSITY AND SIEVE ANALYSIS**

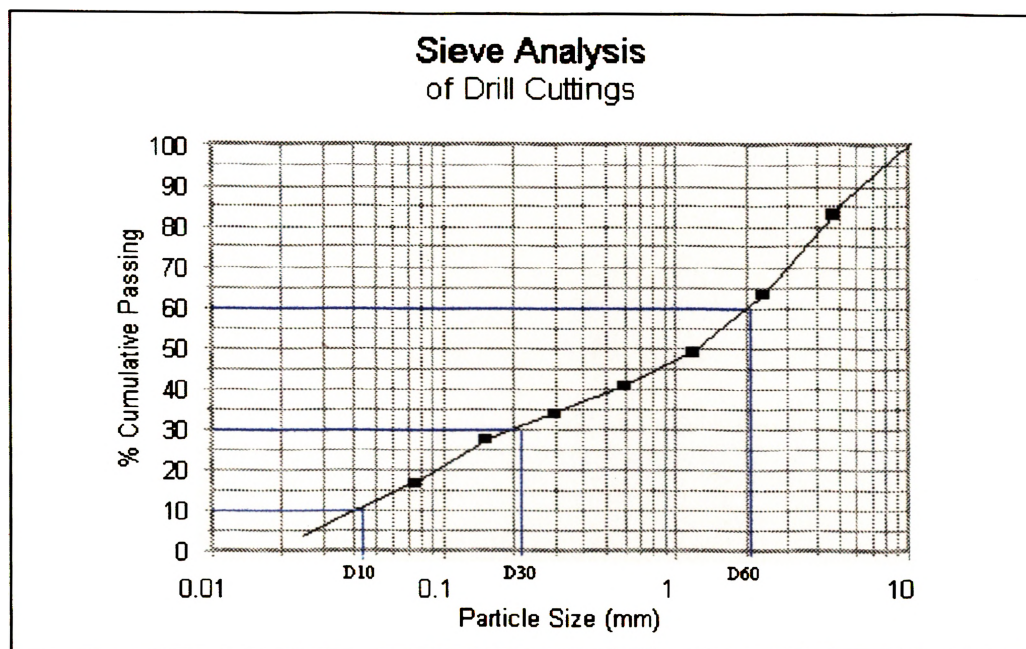
**Table D-I -- Bulk Density Calculations of All Materials**

<b>Material</b>	<b>Beaker Mass (g)</b>	<b>Beaker Volume (mL)</b>	<b>Beaker + Material Mass (g)</b>	<b>Material Mass (g)</b>	<b>Density (g/mL) or (g/cc)</b>
<b>ANFO</b>	173	500	612	439	0.88
<b>1/8 in. minus filter Sand</b>	210	500	946	736	1.47
<b>1/8 – 1/4 in. Gravel</b>	173	500	895	722	1.44
<b>1/4 – 3.4 in. Pea Gravel</b>	210	500	929	719	1.44
<b>Drill Cuttings</b>	210	500	1036	826	1.65

**Table D - II Sieve Analysis of Drill Cuttings**

Total Mass of Sample  
248.5 g

Sieve #	Sieve Size (mm)	Grams Held	Grams Passed	Percent Cumulative Passing
#4	4.75	42	206.5	83.10
#8	2.36	49.5	157	63.18
#16	1.18	35.1	121.9	49.05
#30	0.6	20.8	101.1	40.68
#50	0.3	16.9	84.2	33.88
#100	0.15	16.3	67.9	27.32
#200	0.075	27.1	40.8	16.42
Pan		40.8		
		<u>248.5</u>		



D10 = 0.044  
D30 = 0.203  
D60 = 2.05

**Uniformity Coeff.**  
U = 46.59091  
**Coefficient of Curvature**  
Cc = 0.456863



## **REFERENCES**

- Atlas Powder Company, "Explosives and Rock Blasting," Atlas Powder Company, Dallas, TX, 1987.
- Brown, John, AMAX Coal, Personal Conversation, 15 April 1997.
- Chiappetta, R.F., Srihari, H.N., Worsey, P.N., "Design of Overburden Casting by Blasting -- Recent Developments," *Journal of Mines, Metals & Fuels*, Vol. 38, No. 9, pp. 194-208, September 1990.
- Department of Army, Corp of Engineers, "Systematic Drilling and Blasting for Surface Excavations," Department of Army, Washington D.C., March 1972.
- Du Pont, "Blaster's Handbook," 16<sup>th</sup> Edition, Du Pont Company and the Explosives Product Division, Wilmington, Delaware, 1977.
- Dupree, Paul D., "Applied Drilling and Blasting Technique for Blast Casting at Trapper Mine, Craig, Colorado," Proceedings of the Twelve Conference on Explosives and Blasting Technique, Society of Explosives Engineering, Atlanta, Georgia, 1986.
- Favreau, R. F., Elliot, M., and Schneider, D., "Effect of Inclined Boreholes on the Quality of Blast Results in Coal Mining – Comparison between Field and Simulated Results," Proceedings of the Fourteenth Conference on Explosives and Blasting Technique, Society of Explosives Engineering, Anaheim, California, 1988.
- Konya, C. J., and Davis, G. J., "The Effects of Stemming Consist on Retention in Blastholes," Proceedings of the Fourth Conference on Explosives and Blasting Technique, Society of Explosives Engineering, New Orleans, Louisiana, February 1978.
- Konya, C. J., Otuonye, F. O., and Skidmore, D. R., "Airblast Reduction from Effective Blasthole Stemming," p. 145-156, Proceedings of the Eighth Conference on Explosives and Blasting Technique, Society of Explosives Engineering, New Orleans, Louisiana, January 1982.
- Konya, C. J., and Walter, E. J., "Surface Blast Design," Prentice Hall Publishing, Englewood, New Jersey, 1990.
- Konya, C. J., and Walter, E.J., "Seminar on Blasting and Overbreak Control," Rock Blasting, U.S. Department of Transportation, May 1985.
- Langefors, U., and Kihlström, B., "Rock Blasting," John Wiley and Sons, Inc., New York, 1963.

- Leader, Jack C., "The Manufacture of Wet Hole Shot Bags," Proceedings of the Seventh Conference on Explosives and Blasting Technique, Society of Explosives Engineering, Phoenix, AZ, 1981.
- Olofsson, Stig O, "Applied Explosives Technology for Construction and Mining," Applex Publishing, ÄRLA, Sweden, 1988.
- O'Meara, Richard, "Blasting Over 40 ft. Toe Burden – Case Studies Outlining Modern Planning Techniques," p. 377-388, Proceedings of the Twentieth Conference on Explosives and Blasting Technique, Society of Explosives Engineering, Austin, Texas, 1994.
- Rollins, R.R., Givens, R.W., "High Power Energy Casting," Proceedings of the Fourteenth Conference on Explosives and Blasting Technique, Society of Explosives Engineering, Anaheim, CA, 1988.
- Rossow, D.E., "Expandable Packaged ANFO in the Field," Proceedings of the Eleventh Conference on Explosives and Blasting Technique, Society of Explosives Engineering, San Diego, California, 1985.
- Stachura, Virgil J., and Cumerlato, Calvin L., "Highwall Damage Control Using Pre-Splitting with Low Density Explosives," Proceedings of the Twenty First Conference on Explosives and Blasting Technique, Society of Explosives Engineering, Nashville, TN, 1995.
- Trudinger, J.P., "An Approach to the Practice of Pre-Splitting in Anisotropic Rock Masses," *Bulletin of the Association of Engineering Geologists*, 10 (3), pp. 161-171, 1973.
- USBM, Explosives Consumption Survey, 1995.
- Worsey, P.N., "Geotechnical Factors Affecting the Application of Pre-Split Blasting to Rock Slopes," Ph.D. Thesis, University of Newcastle-upon-Tyne, UK, August 1981.

## VITA

Michael Wilkins was born on the 27<sup>th</sup> of December 1972 in St. Charles, Missouri. After receiving his primary and secondary education in the Francis Howell public school system of St. Charles, he studied at the University of Missouri-Rolla, in Rolla, Missouri. He received a Bachelor of Science in Geological Engineering from the University of Missouri-Rolla in May of 1995, graduating *summa cum laude*.

Following graduation, Michael accepted a summer intern position with Meridian Oil of Houston, TX during the summer of 1995. After the completion of the internship, Michael started graduate work in Mining Engineering at Montana Tech of the University of Montana in Butte, Montana.

Due to his interest in the Explosives Industry, Michael returned to the University of Missouri-Rolla in the summer of 1996 to continue his graduate work in Mining Engineering with an appointment at the Rock Mechanics and Explosives Research Center. Upon returning to Rolla, Michael spearheaded the revitalization of the local chapter of Alpha Chi Sigma, the social/professional chemical fraternity, and he has always been a proud and active member of the Kappa Sigma Fraternity, Beta Chi Chapter.

